UNIVERSITA' DEGLI STUDI DI PARMA

DOTTORATO DI RICERCA IN
NEUROSCIENZE

Ciclo XXXI

Extending the lateral grasping network to the mesial wall. Visuo-motor properties of single neurons in area F6 of the macaque's brain

Coordinatore:

Chiar.mo Prof. Vittorio Gallese

Tutor:

Chiar.mo Prof. Leonardo Fogassi

Dottorando: Alessandro Livi

Anni 2015/2018

INDEX

1. Introduction **7**

1.1. Motor and cognitive functions of the lateral grasping network **9**

1.2. Functional organization of the mesial premotor cortex **14**

1.3. Anatomo-functional relationship between dorsolateral and mesial premotor cortex **15**

1.4. Aims of the study **16**

2. Material and methods **18**

2.1. Subjects and surgery **18**

2.2. Apparatus and behavioral paradigm **18**

2.3. Recording and intracortical microstimulation techniques **22**

2.4. Recording of behavioral events and definition of epochs of interest **24**

2.5. Electromyographic (EMG) recordings **25**

2.6. Single unit analysis **25**

2.7. Population analysis **27**

2.8. Heat maps construction **28**

2.9. Correlation analyses **28**

2.10. Decoding analyses **29**

2.11. Anatomical localization of the recorded regions **31**

3. Results **32**

3.1. Experiment 1 **36**

Purely motor neurons **37**

Visually-triggered neurons **39**

Neuronal properties and dynamics in mesial (F6) and ventral (F5) premotor cortex **44**

3.2. Experiment 2 **50**

Monkeys react differently to the same cue depending on task context **50**

Agent- based representation of manual actions and graspable objects at the single neuron level **51**

Self-biased agent-based representation of reaching- grasping actions **52**

Agent-based representation of graspable objects **56**

Object-related neuron activity is strictly constrained to the monkey's peripersonal space **59**

Agent-based population codes dynamically emerge from object presentation to action execution **61**

4. Discussion **65**

Conclusions **72**

5. References

Acknowledgments

Part of the thesis is a pre-copyedited, author-produced version of an article accepted for publication in Cerebral Cortex following peer review. The version of record is "Extending the Cortical Grasping Network: Pre-Supplementary Motor Neuron Activity During Vision and Grasping of Objects", Cerebral Cortex, Volume 25, Issue 12,1 December 2016, Pages 4435-4449 is available online at: https://doi.org/10.1093/cercor/bhw315

1. INTRODUCTION

The cortical control and organisation of visually guided grasping actions in primates depends mainly on the primary motor cortex and on a network of reciprocally interconnected parietal and premotor areas lying on the dorsolateral portion of the cerebral hemispheres (Figure 1) (Rizzolatti & Luppino, 2001; Grafton, 2010; Davare *et al.*, 2011; Kaas & Stepniewska, 2016b). In the last three decades, the premotor cortex (PM) of primates has been subject to increasing scientific interest for its crucial role not only in planning and organizing movement (Hoshi & Tanji, 2007), but also in several perceptual and socio-cognitive functions (Cisek & Kalaska, 2010; Rizzolatti *et al.*, 2014).

Monkey neurophysiological and neuronatomical studies have been crucial to drive our current understanding of the manifold functions and anatomical circuitries linking sensory processing, in the parietal lobe, with a direct recruitment of motor representations of self and other's grasping actions, graspable objects and operational space around us. The most recent views support the idea of close sensorimotor loops (Cisek, 2007; Cisek & Kalaska, 2010), or "perception-action" cycles (Fuster, 2015), in which perception and action are intimately interrelated aspects which cannot be clearly distinguished neither in the anatomical/spatial nor in the temporal domain. Indeed, many categories of neurons have been described, each associated to a specific function, such as motor goal coding, sensorimotor transformations, or action recognition, and deemed to be unevenly distributed into different premotor sectors. All these classes of neurons can become active in response to external sensory information, providing an automatic translation of sensory stimuli into their potential behavioral meaning, and hence generating representations of several potential motor actions. The selection of a given action may derive from a competition process among alternatives, with prefrontal regions and basal ganglia biasing this process based on a variety of internal and external information (Cisek, 2007).

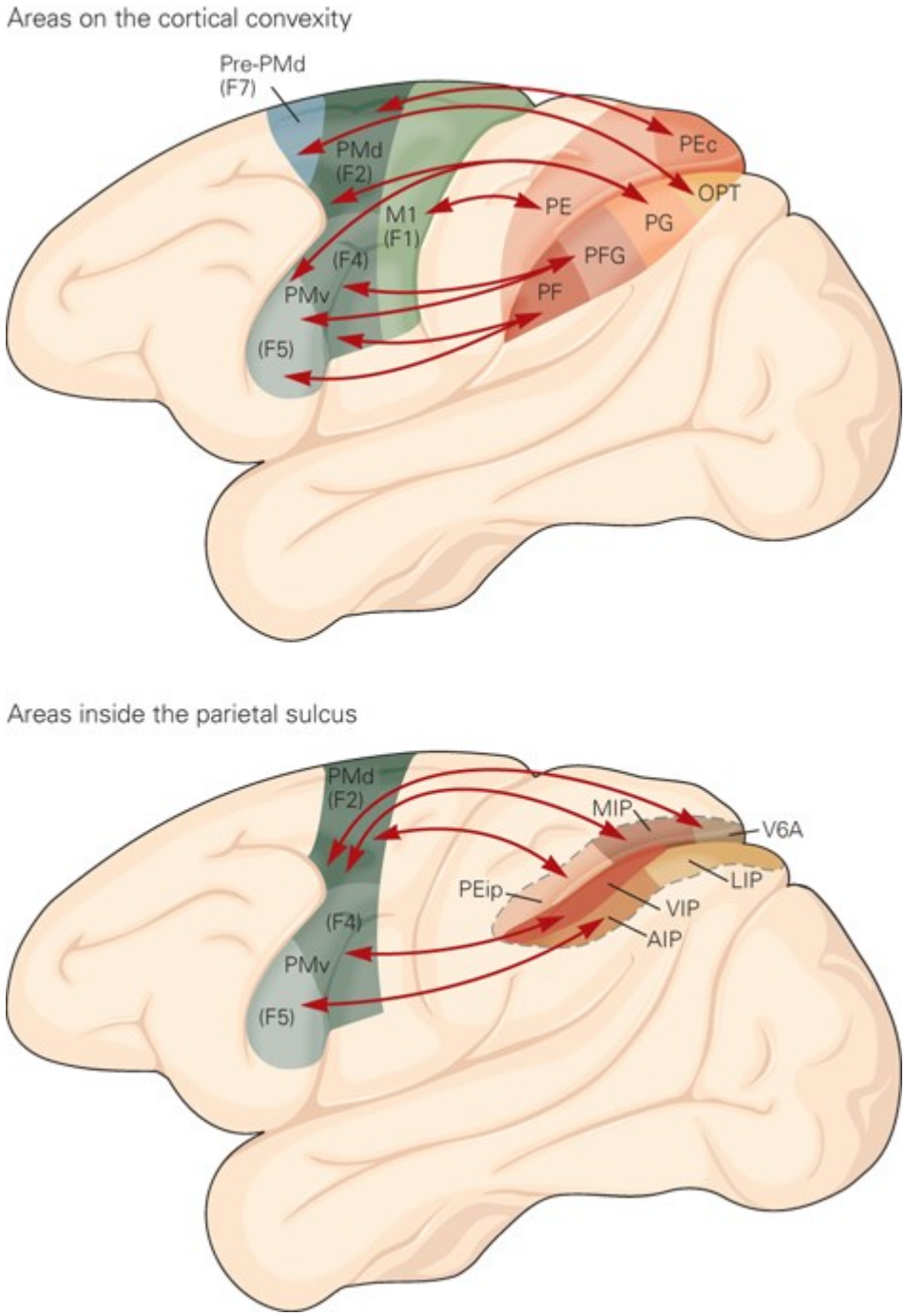

Figure 1. Sketch of parieto-frontal connections of the macaque's brain. The figure shows lateral views of a macaque brain. Motor cortex has been represented with different tones of green to highlight the cytoarchitectonic organization of this region. Similarly, citoarchitectonic subdivision of the parietal cortex have been indicated in tones of red. PMd, dorsal premotor; PMv, ventral premotor; MIP, medial intraparietal area; LIP, lateral intraparietal area; VIP, ventral intraparietal area; AIP, anterior intraparietal area. All the remaining acronyms defined as in (Pandya & Seltzer, 1982). Figure from (Kandel, 2012).

Most of the existing literature on the neural underpinning of sensorimotor processes focused on the ventral and dorsal premotor cortex: these regions are tightly anatomically linked with parietal regions, which provide sensory

information to be matched with the premotor action plans (Borra *et al.*, 2017), whereas areas of the mesial wall, and in particular the pre-supplementary motor area F6, are deemed to have a main role in making a bridge between prefrontal and dorso-lateral premotor area, contributing to triggering and sequencing motor behaviors with only modest parametric selectivity for the details of the selected motor plans (Rizzolatti & Luppino, 2001).

With a series of neurophysiological experiments in monkeys based on the same tasks and animals previously used to study area F5 sensorimotor properties, the present study provides new data suggesting area F6 should be included as a node of an extended, not just lateral, cortical grasping network. Furthermore, data suggests area F6 is involved in a variety of motor-based cognitive function, such as agent-based action representation and contextually-driven action prediction.

1.1 MOTOR AND COGNITIVE FUNCTIONS OF THE LATERAL GRASPING NETWORK

Neurophysiological studies in the monkey have revealed that the anterior intraparietal area (AIP) (Sakata *et al.*, 1995; Baumann *et al.*, 2009), the posterior parietal area V6A(Fattori *et al.*, 2012; Fattori *et al.*, 2017), the ventral premotor area F5 (Murata *et al.*, 1997; Raos *et al.*, 2006; Fluet *et al.*, 2010; Bonini *et al.*, 2014b; Vargas-Irwin *et al.*, 2015) and the ventro-rostral portion of the dorsal premotor area F2 (Raos *et al.*, 2004; Vargas-Irwin *et al.*, 2015) host visuomotor neurons that discharge during both the visual presentation of target objects and the execution of reaching-grasping actions. These areas form a rich set of parieto-frontal circuits that underlie the visuomotor transformations of objects properties into the most appropriate motor acts to interact with them (Maranesi *et al.*, 2014a).

Studies on the forelimb field of PMv (areas F4 and F5) and of the adjacent ventro-rostral sector of the dorsal premotor area F2 (F2vr) demonstrated the existence of several classes of neurons with distinct functional roles. The most obvious type of cells one would expect to find in a motor area are certainly represented by “purely motor neurons” (Figure 2, Unit A): they respond only during

the execution of hand, hand-and-mouth or arm motor acts, and are deemed to code "motor goals", such as the direction of reaching (Kakei *et al.*, 2001) or the getting an object (Rizzolatti *et al.*, 1988; Raos *et al.*, 2006; Bonini *et al.*, 2010), even regardless of the specific movement sequence required to attain the goal (Umilta *et al.*, 2008). In addition, hand-related neurons can also specify the type of grip to be employed for grasping (Rizzolatti *et al.*, 1988; Raos *et al.*, 2004; Raos *et al.*, 2006; Bonini *et al.*, 2012). Thus, PM purely motor neurons encode a rich variety of details of the planned action, allowing to accurately decode motor parameters from neuronal activity (Serruya *et al.*, 2002; Gallego *et al.*, 2017).

Interestingly, besides purely motor neurons, many PM cells show visuo-motor properties. "Peripersonal" neurons, reported in areas F4 (Gentilucci *et al.*, 1983; Fogassi *et al.*, 1996; Graziano, 1999) and F2vr (Fogassi *et al.*, 1999), are a class of bimodal neurons characterized by the presence of a somatosensory receptive field located on a specific body part (e.g. hand, arm, trunk or face) which encodes not only objects that contact the body but also those approaching it by entering into the 3D projection of the tactile receptive field in the peripersonal visual space anchored to it. Since intracortical microstimulation of the premotor region hosting peripersonal neurons evokes arm and face avoidance behaviors, whereas its pharmacological inhibition reduces behavioural responsiveness to looming stimuli (Cooke & Graziano, 2004), the most reliable interpretation of peripersonal neuron activity is that it encodes potential reaching or avoidance behaviors related to stimuli entering in the subject's peripersonal (operative) space.

Another class of PM visuomotor neurons is constituted by "canonical neurons", which respond to the visual presentation of graspable objects (Figure2, Unit B) (Murata *et al.*, 1997; Raos *et al.*, 2006). Similar neurons were previously described in the parietal area AIP (Sakata *et al.*, 1995), which is tightly anatomically connected with area F5 (Borra *et al.*, 2008). Furthermore, reversible inactivation of both AIP (Gallese *et al.*, 1994) and F5 (Fogassi *et al.*, 2001) significantly impairs visually guided object grasping, providing causal evidence of a critical role of the AIP-F5 circuits in transforming the visual representation of object physical properties into the appropriate, potential motor plan to be used for interacting with the object. Recent studies with simultaneous recording from area AIP, F5 and F1 provide elegant dynamic pictures of the visuomotor transformation process

(Schaffelhofer & Scherberger, 2016), and further support the idea that causal functional relationships between these nodes of the network causes sensory information in AIP to be turned into planned actions in area F5, which finally recruits the "common motor output" by means of its direct projections to the spinal cord (Borra *et al.*, 2010) and, most importantly, via its direct link with the primary motor area F1(Kraskov *et al.*, 2011; Schaffelhofer & Scherberger, 2016). Neurons with canonical-like properties have been also found in the dorsal premotor cortex (area F2vr) (Raos *et al.*, 2006) as well as in the parietal area V6A (Gamberini *et al.*, 2015), which is anatomically connected with F2 (Marconi *et al.*, 2001). These findings clearly demonstrate that the AIP-F5 and V6A-F2vr form parallel circuits for the visuomotor transformations underlying object grasping: the simple sight of a visually presented object ("object affordance) produces the activation of the neuronal motor repertoire suitable to take possession of it.

Another class of cell first described in the ventral premotor area F5 is the so called "mirror neurons" (MNs, Figure 2, Unit C). MNs encode motor actions both when they are actively performed by the monkey and when they are observed, done by another agent (Gallese et al. 1996; Rizzolatti et al. 1996). Hence, they represent "action" in an agent-shared motor format, encoding motor goals both when these are attained by the subject or by another agent. Several regions in the primates' brain host neurons that encode both one's own and others' actions (Giese & Rizzolatti, 2015; Bonini, 2016; Bruni *et al.*, 2018), hence generating a putatively agent-invariant code for actions (Sinigaglia & Rizzolatti, 2011), which is deemed to be at the basis of several cognitive functions and social interaction skills (Bonini & Ferrari, 2011; Rizzolatti & Sinigaglia, 2016). Neurons with mirror properties have also been reported in other animal species and may subserve a large variety of socio-cognitive functions (Bonini & Ferrari, 2011). They can exploit contextual information to generate predictive representations of what others' are going to do (Fogassi *et al.*, 2005; Bonini *et al.*, 2010; Maranesi *et al.*, 2014b). Most of these neurons have been also shown to be strongly influenced by specific contextual factors, such as space (Caggiano *et al.*, 2009), value (Caggiano *et al.*, 2012), social stimuli (Yoshida *et al.*, 2012) and non-social visual or auditory cues (Cisek & Kalaska, 2004; Fogassi *et al.*, 2005; Bonini *et al.*, 2010; Fluet *et al.*, 2010; Maranesi

et al., 2014b) leading to many hypotheses on their possible role in daily life situations.

Recent findings (Bonini *et al.*, 2014b) showed a more complex picture with the two types of visuomotor neurons, canonical and mirror neurons, being not completely separated. Indeed, area F5 hosts two types of neurons with canonical properties: most of them fit with the classical description of "canonical neurons", showing object presentation responses strictly constrained to the monkey's peripersonal (pragmatic) space, likely playing a role in the transformation of the "graspability" of an object into the appropriate motor plan to interact with it (Fogassi *et al.*, 2001), whereas others, called 'canonical-mirror' neurons, can respond to the presentation of objects in the extrapersonal space, but virtually all of them also show a response to action observation, suggesting they might generate object-triggered, predictive representations of the upcoming action of the observed agent. This mixed selectivity is linked with another intriguing property of premotor neurons: that of specifically mapping other's observed action by activating their corresponding representation in the observer's brain.

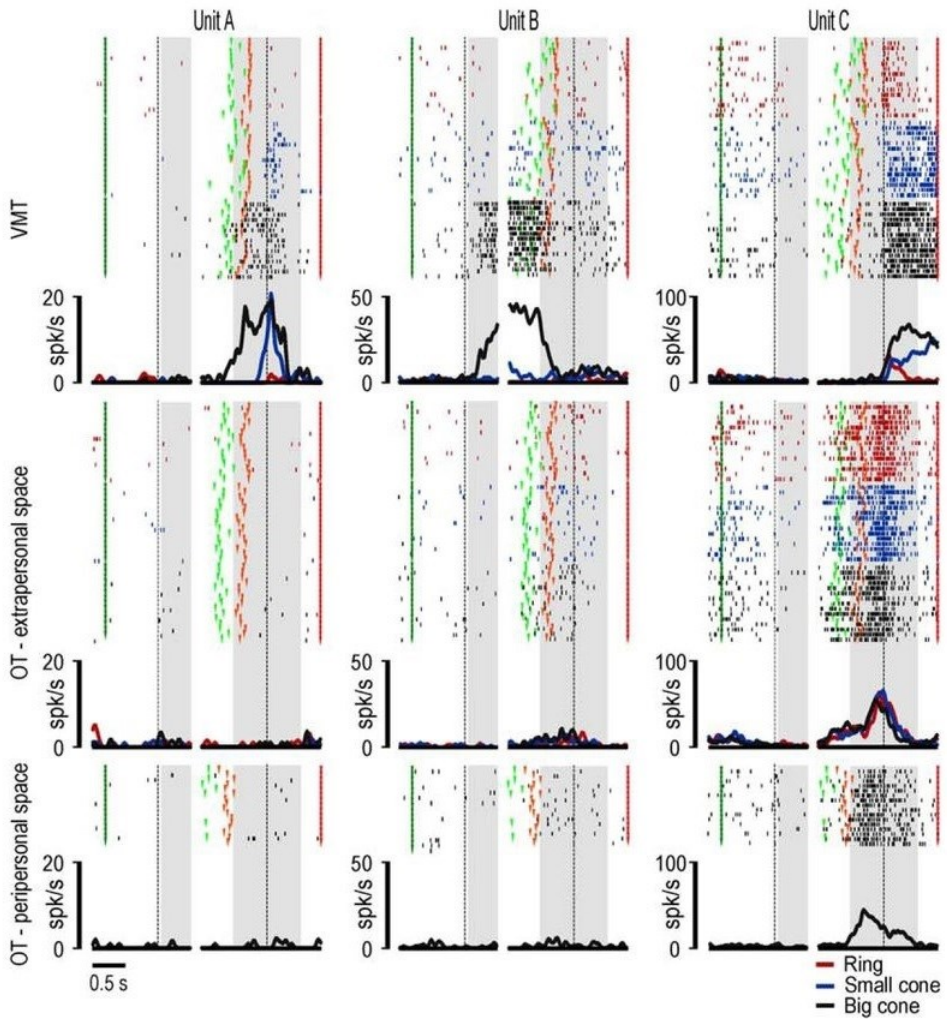

Figure 2. Area F5 single unit examples. Example of a purely motor neuron (Unit A), a canonical neuron (Unit B), and a mirror neuron (Unit C). For each neuron, the gap in the histogram and rastergram is used to indicate that the activity on its left side has been aligned on object presentation (first vertical dashed line in the left panel), whereas that on its right side is aligned on the pulling onset (second vertical dashed line in the right panel) of the same trial. The gray shaded areas represent the time windows used for statistical analysis of neuronal response. Markers: dark green, cue sound onset; light green, cue sound offset (go signal); orange, detachment of the hand from the starting position (reaching onset); red, reward delivery at the end of the trial. The same markers have been used to identify the behavioral event of interest of both the visuomotor and observation tasks. Figure and caption from (Bonini *et al.*, 2014b)

1.2 FUNCTIONAL ORGANIZATION OF THE MESIAL PREMOTOR CORTEX

Area F6 is lying on the anterior part of the mesial wall of area 6. Intracortical microstimulation studies in monkeys have demonstrated that this area controls complex multi-joint forelimb movements, with higher current intensity threshold than the adjacent, caudal area F3. Pioneering neurophysiological studies performed in naturalistic settings (Rizzolatti *et al.*, 1990a) have shown that area F6 neurons discharged during reaching-grasping movements, but "did not appear to be influenced by how the objects were grasped nor by where they were located". These findings suggested that F6 "plays a role in the preparation of reaching-grasping arm movements and in their release when the appropriate conditions are set" (Rizzolatti *et al.*, 1990a) but it is not involved in the encoding of specific motor aspects, such as object/grip features. Along the same lines, subsequent neurophysiological studies on area F6 focused on fairly simple limb movements whose temporal/sequential organisation (Figure 3), initiation and stopping were instructed by sensory cues (Tanji & Hoshi, 2001; Nachev *et al.*, 2008), but they did not investigate manipulative actions, thus leaving unknown whether and to what extent F6 is involved also in visuomotor processing of objects for grasping.

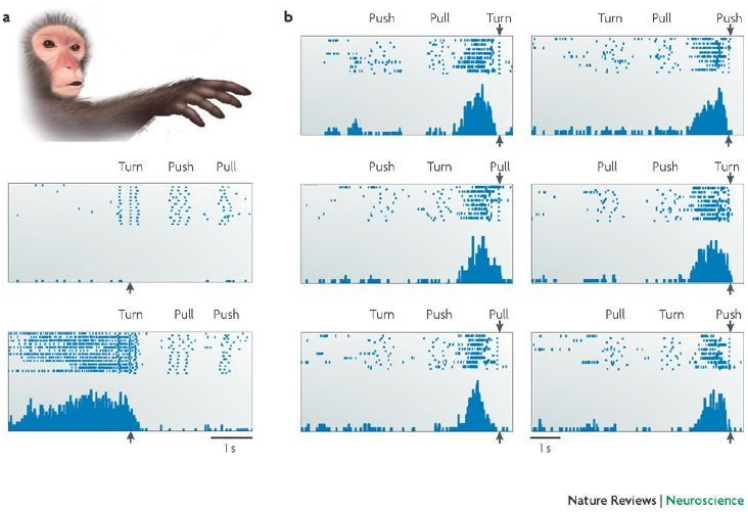

Figure 3. Neurons of area F6 related to movement sequences. In a is represented a monkey executing a movement with the hand. Below the activity of one example neuron while the animal is performing sequences of movement. This neuron is encoding the "turn" movement only in one of the sequences. B is an example of neuron encoding the third movement in a sequence, even if the type of movement changed across the task condition. Figure from (Nachev *et al.*, 2008).

Area F6 might also constitute a crucial node of the cortical mirror neuron system, both in humans (Nachev *et al.*, 2008; Mukamel *et al.*, 2010) and monkeys (Yoshida *et al.*, 2011; Isoda & Noritake, 2013). Indeed, recent studies indicate that area F6 plays a role in a number of motor-based social and cognitive functions, such as switching from automatic to controlled actions (Isoda & Hikosaka, 2007), encoding of self and other's action (Yoshida *et al.*, 2011), and social error monitoring (van Schie *et al.*, 2004; Yoshida *et al.*, 2012; Falcone *et al.*, 2017). Furthermore, the strong connections of this area with area F5 (Luppino *et al.*, 1993; Gerbella *et al.*, 2011) support a mutual role of these two nodes in similar functions.

Yoshida and coworkers tested F6 neurons with a role-reversal arm-reaching task in which two monkeys alternatively played the role of actor and partner. They found three main types of neurons: "partner-type" neurons, encoding selectively others' action; "self-type" neurons, encoding one's own action; and "mirror-type" neurons, encoding both one's own and others' action. These findings demonstrated the existence of an agent-based representation of reaching actions in the mesial frontal cortex, which may be critical during interaction with others. Indeed, the pre-supplementary motor cortex has been recently identified as a key node of a brain network dedicated to processing observed social interactions (Sliwa & Freiwald, 2017).

1.3 ANATOMO-FUNCTIONAL RELATIONSHIP BETWEEN DORSOLATERAL AND MESIAL PREMOTOR CORTEX

One of the most well-established assumptions underlying the relationship between mesial and dorso-lateral premotor cortices is that motor representations encoded in the lateral grasping network need to be selected, triggered or inhibited in order to appropriately turn them into action (Rizzolatti & Luppino, 2001). This latter function is typically associated with the pre-supplementary motor cortex, and in particular to area F6 as defined in macaques (Matelli *et al.*, 1991), considered to be a "prefronto-dependent" region as opposed to "parieto-dependent" regions in the more caudal part of the dorso-lateral premotor cortex (Rizzolatti & Luppino, 2001).

The functional properties of area F6 described above are grounded on its anatomical connectivity. Area F6 does not only represents the crucial bridge between prefrontal areas (i.e. area 46v) and the PMv (particularly area F5) (Gerbella *et al.*, 2011; Gerbella *et al.*, 2013), but it also receives some projections from the superior temporal sulcus and the inferior parietal areas PF/PFG and (Luppino *et al.*, 1993; Gerbella *et al.*, 2017). This pattern of connections, and the anatomo-functional relationships with other nodes of the cortical grasping network, suggest that the functional properties and related roles of area F6 in object grasping may have been underestimated, and in any case no direct comparative study has ever been performed to directly assess the relative contribution of F6 and F5 in transitive grasping actions.

1.4 AIMS OF THE STUDY

In this study, we investigated the visual and motor properties of F6 neurons by employing multiple execution and observation tasks, suitable to verify neuronal responses to visually presented objects in different contexts, during action execution (including possible grip selectivity), as well as to the observation of others' action. Based on the existing knowledge about area F6 anatomo-functional organization, we first aimed at establishing the visuomotor properties of F6 neurons tested while monkeys were performing a visuomotor Go/No-Go reaching-grasping task (Experiment 1), then we further investigated the possible involvement of this area in the representation of other's action and action contexts (i.e. objects as potential targets for self or others' action).

More specifically, Experiment 1 investigated whether and to what extent F6 neurons are involved in visuomotor processing of objects for grasping. By leveraging on the same tasks and animals previously employed to characterize the activity of the hand sector of area F5 (Bonini *et al.*, 2014b; Maranesi *et al.*, 2015), we were able to directly compare the functional properties of the two regions.

Experiment 2 aimed at investigating the neuronal mechanisms for agent-based motor representation of real solid objects and, most importantly, their

possible link with self- and other-action coding, by requiring monkeys to simply observe, in addition to perform, the same visuomotor task used in Experiment 1.

2. MATERIAL AND METHODS

2.1 SUBJECTS AND SURGERY

Experiments were carried out on one Macaca nemestrina (M1, male, 9 kg) and one Macaca mulatta (M2, male, 7 kg). Before recordings, monkeys were habituated to sit in a primate chair and to interact with the experimenters. They were then trained to perform the visuomotor tasks described below using the hand contralateral to the hemisphere to be recorded. When the training was completed, a head fixation system was implanted under general anaesthesia (ketamine hydrochloride, 5 mg/Kg i.m. and medetomidine hydrochloride, 0.1 mg/Kg i.m.), followed by postsurgical pain medications. Surgical procedures were the same as previously described (Bruni *et al.*, 2015). All experimental protocols complied with the European law on the humane care and use of laboratory animals (directives 86/609/EEC, 2003/65/CE, and 2010/63/EU), they were authorized by the Italian Ministry of Health (D.M. 294/2012-C, 11/12/2012), and approved by the Veterinarian Animal Care and Use Committee of the University of Parma (Prot. 78/12, 17/07/2012 and Prot. 91/OPBA/2015).

2.2 APPARATUS AND BEHAVIORAL PARADIGM

Both monkeys were trained to perform, in different blocks, 1) a Go/No-Go execution task (Execution, Figure 3a), 2) an Observation task carried out in the monkey Peripersonal space (Observation, Figure 3b), and 3) an Observation task carried out in the monkey Extrapersonal space (Extrapersonal, Figure 3c). We used a custom-made apparatus (Figure 3 d-f) allowing us to rapidly shift from one task condition to the other, so that all tasks could be performed within the same session (Bonini *et al.*, 2014b; Maranesi *et al.*, 2015; 2017). All tasks were performed by the monkey or experimenter with the hand contralateral to the recorded hemisphere. In the Execution task, the monkey, was seated on a primate chair in front of a box,

shown in Figure 3d from the monkey's point of view. The box was divided horizontally into two sectors by a half-mirror: the upper sector contained a small black tube with a white light-emitting diode (LED) that could project a spot of light on the half-mirror surface; the lower sector contained a sliding plane hosting three different objects.

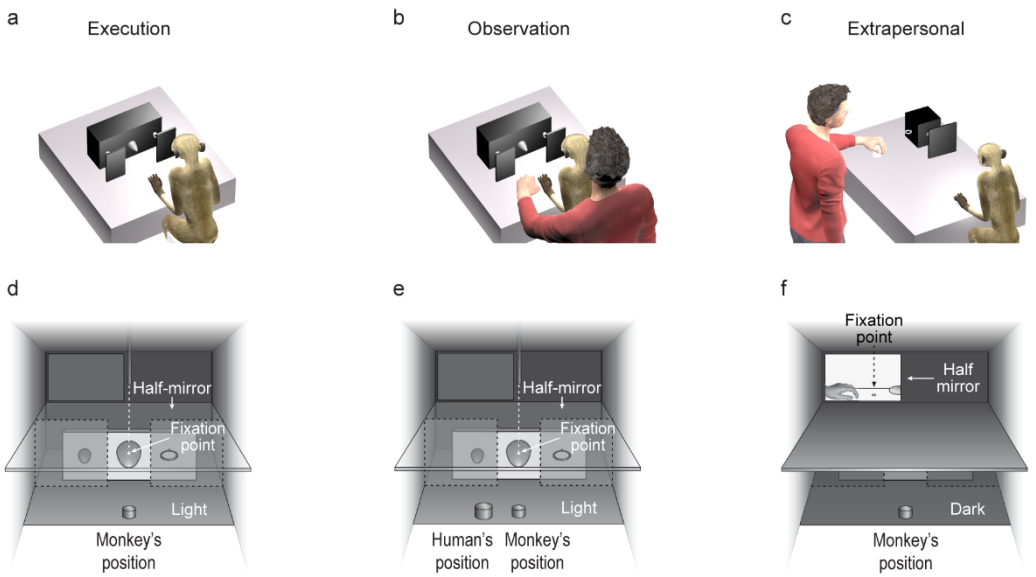

Figure 3. Setup configurations for the behavioral tasks. The behavioral setup allowed three different configurations for performing the Executions task (a), the Observation task (b) and the Extrapersonal task (c). In (a), the animal alone faces the box and perform the task by grasping, or refraining from grasping, the visually presented object, depending on the instructive cue. In (b) the experimenter stands on the back of the animal and performs the task using the same arm used by the animal during task execution (the one contralateral to recorded hemisphere). In the meantime, the animal keeps its hand always still on the starting position. In (c) the experimenter is far from the animal and is performing the task allowing the animal to see the scene from a side-view. Box and apparatus seen from the monkey's point of view settled for (d) the Execution task, (e) the Observation task and (f) the Extrapersonal task. The half-mirror allowed the animal to see the target only when the lower sector of the box was illuminated (object presentation). The fixation point was set to be in the center of each target. Human's position indicates an additional manipulandum placed 10 cm on the side of the monkey's hand during the Observation task. In the extrapersonal task, the half mirror allowed the animal to see (from a side-view) the object and subsequently the experimenter's action only when the light was turned on (object presentation). The fixation point was located in between the hand's starting position and the target object. The action was executed in the hemifield and with the hand contralateral to the recorded hemisphere.

When the LED was turned on (in complete darkness), the half-mirror reflected the spot of light so that it appeared to the monkey as located in the lower sector (fixation point), in the exact position of the center of mass of the not-yet-

visible target object. The objects – a ring, a small cone and a big cone – were chosen because they afforded three different grip types, as follows: hook grip (in which the index finger enters the ring); side grip (performed by opposing the thumb and the lateral surface of the index finger); whole-hand prehension (achieved by opposing all the fingers to the palm). Objects were presented, one at a time during different experimental trials, through a 7 cm opening located on the monkey's sagittal plane at a reaching distance from its hand starting position. A stripe of white LEDs located on the lower sector of the box allowed us to illuminate it during specific phases of the task. Note that, because of the half-mirror, the fixation point remained visible in the middle of the object even when the lower sector of the box was illuminated.

The task included three basic conditions, as illustrated in Figure 4: grasping in the light, grasping in the dark and a no-go condition. Each of them started when the monkey held its hand on a fixed starting position, after a variable intertrial period ranging from 1 to 1.5 seconds from the end of the previous trial.

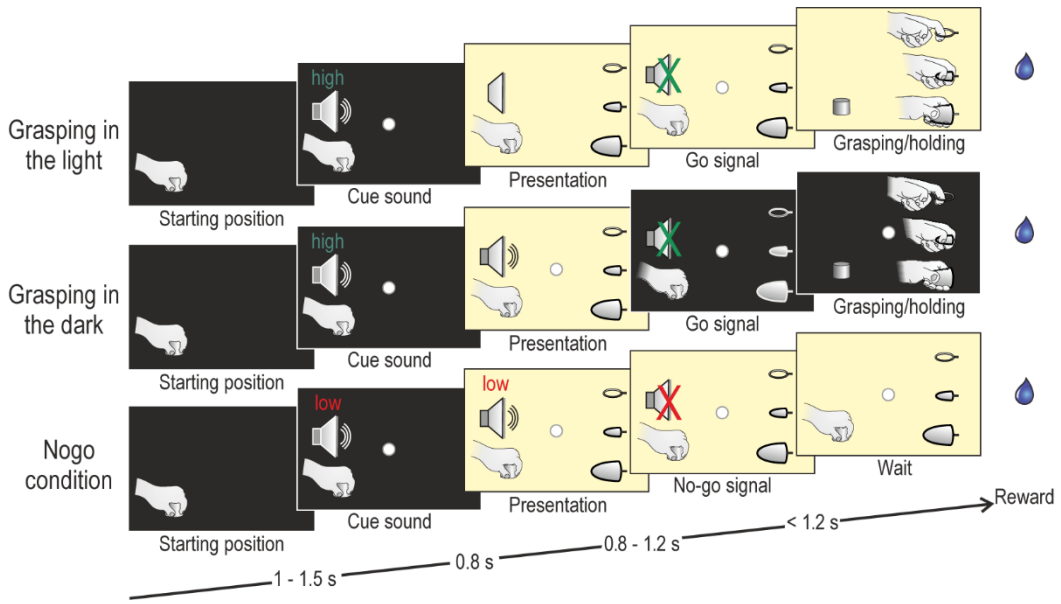

Figure 4. Temporal sequence of task events. Each trial started when the monkey, with its hand contralateral to the recorded hemisphere in a starting position, engaged fixation in complete darkness. A high (Go cue) or low (No-Go cue) tone was presented (Cue Sound) and remained on during the subsequent object-presentation phase (Presentation). When the sound stopped (Go/No-Go signal), the agent (monkey or experimenter) had to reach, grasp, and pull the target (Go trial, either Grasping in the light or dark) or to remain still (No-Go trial).

Grasping in the light. The fixation point was presented and the monkey was required to start fixating it within 1.2s. Fixation onset resulted in the presentation of a cue sound (a pure high tone constituted by a 1200 Hz sine wave), which

instructed the monkey to grasp the subsequently presented object (go-cue). After 0.8s the lower sector of the box was illuminated and one of the objects became visible. Then, after a variable time lag (0.8-1.2s), the sound ceased (go-signal), at which point the monkey had to reach, grasp and pull the object within 1.2s. It then had to hold the object steadily for at least 0.8s. If the task was performed correctly without breaking fixation, the reward was automatically delivered (pressure reward delivery system, Crist Instruments, Hagerstown, MD).

Grasping in the dark. The entire temporal sequence of events in this condition was identical to that of grasping in the light. However, when the cue sound (the same high tone as in grasping in the light) ceased (go signal), the light inside the box was automatically switched off and the monkey performed the subsequent motor acts in complete darkness. Note that because the fixation point was visible for the entire duration of each trial, it provided a spatial guidance for reaching the object in the absence of visual feedback. In this paradigm, grasping in the light and grasping in the dark trials were identical and unpredictable until the occurrence of the go signal: thus, action planning was the same in both conditions, and the only difference between them was the presence/absence of visual feedback from the acting hand and the target object.

No-go condition. The basic sequence of events in this condition was the same as in the other go conditions, but a different cue sound (a pure low tone constituted by a 300 Hz sine wave), instructed the monkey to remain still and, when it stopped, to continue fixating the object for 1.2s in order to receive a drop of juice as a reward.

In the Observation task (Figure 3b, 4e) the apparatus, the target objects, all the task stages and conditions were as in the Execution task. However, an experimenter stands on the back of the animal and performs the task using the same arm used by the animal during task execution (the one contralateral to recorded hemisphere). In the meantime, the animal keeps its hand always still on the starting position. Experimenter's hand was placed in a manipulandum 10 cm next to the monkey's hand. The monkey had to remain still with its hand on the initial position and to maintain fixation during both Go and No-Go trials, observing the experimenter grasping or refraining from grasping the target.

The Observation task was also run in the monkey's extrapersonal space (Extra, Figure 3c and 3f), in a separate block of trials. The experimenter performed the task (with the same hand used in the peripersonal space), while the animal looked at the scene from a lateral viewpoint (Bonini *et al.*, 2014b). The apparatus, the target objects and all task stages and conditions were the same as in the other tasks, but in this case the monkey could not reach the target, which was exclusively reachable by the experimenter. The task was presented in the space sector contralateral to the recorded hemisphere (left for M1 and right for M2).

The task phases were automatically controlled and monitored by LabView-based software, enabling the interruption of the trial if the monkey broke fixation, made an incorrect movement or did not respect the task temporal constraints described above. In all these cases, no reward was delivered. After correct completion of a trial, the monkey was automatically rewarded with the same amount of juice in all conditions.

The activity of each neuron was recorded in at least 12 trials for each basic condition. In all sessions we also recorded 12 additional control trials in which the monkey was presented, in complete darkness and with its hand still on the starting position, with the fixation point alone: after a variable time lag (<1s) from fixation onset, the reward was delivered. These trials were used to verify the possible presence of neuronal responses due to mouth movements/reward delivery, which could otherwise be confounded with hand-related activity, particularly during the holding epoch that precedes the reward delivery. Neurons responding specifically to this condition were not considered as task related in the present study.

2.3 RECORDING AND INTRACORTICAL MICROSTIMULATION TECHNIQUE

Neuronal recordings were performed by means of chronically implanted two-dimensional (2D) or three-dimensional (3D) arrays of linear silicon probes with eight recording channels per shaft and a variable number of shafts per probe (Figure 5), as follows: one four-shaft 2D probe in the right hemisphere of M1; one four-

shaft 2D probe and one 3D probe in the left hemisphere of M1; two 3D probes in the right hemisphere of M2. All probes were implanted vertically, approximately 1 mm laterally to the mesial wall. Previous reports provide more details on the methodology of probe fabrication (Herwik *et al.*, 2011), assembly (Barz *et al.*, 2014) and implantation (Barz *et al.*, 2014; Bonini *et al.*, 2014a).

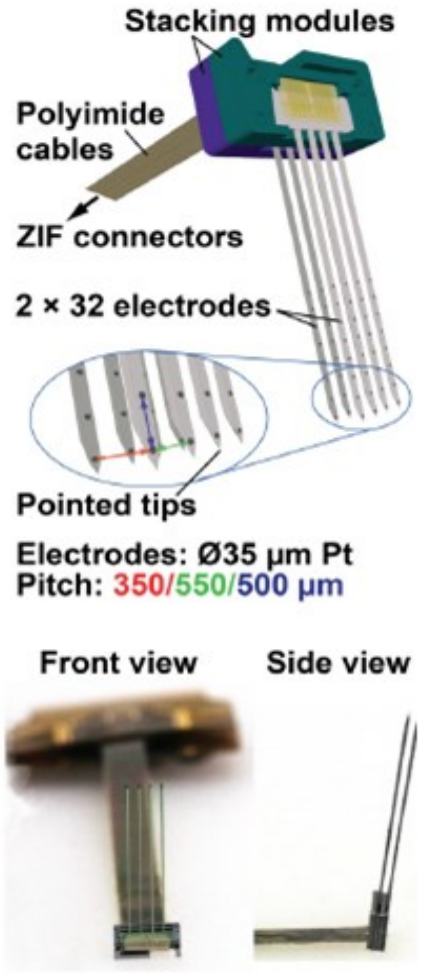

Figure 5. Schematic drawing, features and photograph of a 3d probe. The schematic drawing on the upper part of the figure and the photograph on the bottom illustrate the assembly of 2 2D probes in a 3D configuration. These probes have been implanted in the rostral part of F6 in the left hemisphere of M1 (N=1) and in the right hemisphere of M2 (N=2). For more details on the assembly concept see Barz et al., 2014.

The signal was amplified and sampled at 40 kHz with a 16-channel Omniplex recording system (Plexon, Dallas, TX). Different sets of 16 channels were recorded, only one time, during separate sessions on different days. Online spike sorting was performed on all channels using dedicated software (Plexon), but all final quantitative analyses were performed offline, as described in the subsequent sections. Intracortical microstimulation (ICMS) was performed, in M2, in all recording sites at the end of the recording sessions. Monopolar, biphasic trains of cathodic square wave pulses were delivered through a constant current stimulator (PlexStim, Plexon, Dallas, TX), with the following parameters: total train duration 500 ms, single pulse width 0.2 ms, pulse frequency 300 Hz. The current intensity ranged from 20 to 100 µA and was controlled on an oscilloscope by measuring the voltage drop across a 10 KΩ resistor in series with the stimulating electrode. At each site, ICMS was delivered when the monkey was quiet and relaxed, and those cases in which monkeys performed voluntary movements were not used to establish the stimulation threshold.

Movements were considered to be evoked by ICMS when two experimenters, observing the animal during pulse delivering,

independently and repeatedly identified the same joint displacement or muscular twitch. The threshold was defined as the lowest current intensity capable of evoking movements in 50% plus one of the stimulations delivered (usually four out of six, or five out of eight stimulations).

2.4 RECORDINGS OF BEHAVIORAL EVENTS AND DEFINITION OF EPOCHS OF INTEREST

Distinct contact sensitive devices (Crist Instruments) were used to detect when the monkey (grounded) touched with the hand the metal surface of the starting position or one of the target objects. To signal the onset and tonic phase of object pulling, an additional device was connected to the switch located behind each object. Each of these devices provided a TTL signal, which was used by the LabView-based software to monitor the monkey's performance and to control the generation and presentation of the behavioral paradigm's auditory and visual cue signals.

Eye position was monitored in parallel with neuronal activity with an eye tracking system consisting of a 50Hz CCD video camera provided with an infrared filter and two spots of infrared light. Analog signal related to horizontal and vertical eye position was fed to a computer equipped with dedicated software, enabling calibration and basic processing of eye position signals. The monkey was required to maintain its gaze on the fixation point (tolerance radius 5°) throughout the task, and the eye position signal was monitored by the same LabView-based software dedicated to the control of the behavioral paradigm.

The same software also generated different digital output signals associated with auditory and visual stimuli, the target object presented in each trial, the reward delivery and possible errors made by the monkey during the task (i.e., when the monkey broke fixation). These signals, together with the TTL signals related to the main behavioral events described above, were fed to the Omniplex system to be recorded together with the neuronal activity and subsequently used to construct the response histograms and the data files for statistical analysis.

Single neuron activity was analyzed in relation to the digital signals related to the main behavioral events, by considering the following epochs of interest: 1) baseline, 500 ms before object presentation; 2) object presentation, from 0 to 500 ms after switching on the light; 3) premovement, 500 ms before reaching onset (detachment of monkey's hand from the starting position); 4) reaching-grasping, from reaching onset to pulling onset (of variable duration, calculated on a trial-by-trial basis); 5) object holding, from pulling onset to 500 ms after this event. Note that during baseline the monkey kept its hand on the starting position, was staring at the fixation point and was already aware of whether the ongoing trial was a go or a no-go trial: these features enabled us to assess possible variation in neural discharge specifically linked with the subsequent task stages within the ongoing behavioral set.

2.5 ELECTROMYOGRAPHIC (EMG) RECORDINGS

EMG activity was recorded during separate sessions at the end of the single-neuron recording period. In both monkeys, we used couples of surface electrodes (Ag-AgCl) placed over a proximal (deltoid - DEL) and a distal (extensor digitorum communis - EDC) muscle of the arm contralateral to the hemisphere recorded during the electrophysiological experiments. Data were bandpass filtered between 30 and 500 Hz (4^{th}-order Butterworth), rectified and averaged over trials. The analysis of EMG data was carried out with the same statistic approach described below for neuronal data aligned to object visual presentation and action execution/observation.

2.6 SINGLE UNIT ANALYSIS

The raw signals were high-pass filtered offline (300Hz). Single units were then isolated using principal component and template matching techniques provided by dedicate offline sorting software (Plexon) (Bonini *et al.*, 2014b). After

identification of well-isolated single units we classified neurons significantly activated during specific epoch of interest and task context, depending on the experiment.

In both Experiment 1 and 2 we first tested movement-related response during grasping in the light and grasping in the dark, separately, with a 3 x 4 repeated measures ANOVAs (factors: Object and Epoch). In Experiment 2 the same analysis was applied to test neuronal response to the experimenter's action. Concerning the movement-related responses during the execution task, we classified as 'motor' all neurons showing, at least during the grasping-in-the-dark condition, a significant main effect of the factor Epoch and/or an interaction between the two factors ($p<0.05$), and whose discharge differed from baseline during at least one of the three movement-related epochs (premovement, reaching-grasping, pulling) relative to baseline for at least one of the three target objects (Bonferroni post-hoc tests, $p<0.05$).

We assessed possible responses to *object presentation* relative to baseline in Experiment 1 by considering go and no-go conditions, with a 2 x 3 x 2 repeated measures ANOVA (factors: Condition, Object and Epoch), with a significance criterion of $P<0.05$. Only neurons showing at least a significant effect of the factor Epoch, alone or in interaction with one or both of the other factors, were classified as visually triggered (Bonferroni post-hoc tests, $p<0.05$). In Experiment 1, single-neuron response to the visual presentation of the objects in an additional condition in which a transparent plastic barrier was interposed between monkey's hand and the target was analyzed by means of a 3x2 repeated measures ANOVA (factors: Object, Epoch), with a criterion of $p<0.05$.

The same object-related responses in Experiment 2 were tested with a 3x2 repeated measures ANOVA (factors: Object and Epoch), with the factor Epoch including baseline and object presentation epochs, as defined above. The significance criterion for ANOVAs was set to $p<0.05$, followed by Bonferroni post-hoc test ($p<0.01$) in case of significant interaction effects. Next, in Experiment 2, object-related and action-related neuron responses were further distinguished based on their possible agent selectivity as "self-type", if they responded significantly only during the execution task, "other-type" if they responded significantly only

during the observation task, or "self-and-other type" if they responded significantly during both tasks.

All analyses were carried out using Matlab 2015a and Statistica (Stasoft).

2.7 POPULATION ANALYSIS

Population analyses were carried out taking into account single-neuron responses expressed in terms of mean activity, normalized across all the compared conditions (i.e. for each cell the bin with the highest firing rate across conditions was used to divide bin-by-bin the activity) (Bonini *et al.*, 2010), and analyzed with different repeated measures ANOVAs depending on the conditions to be compared (as described in the figures caption). For each of the recorded neurons, we also calculated the timing of the activity peak. For this purpose, we considered the averaged activity across 12 trials of the same condition in bins of 100 ms, slit forward in steps of 20 ms, within a time window ranging from 500 ms before movement onset to 1 second after this event: the timing associated with the highest among all the obtained values was considered the peak of activity timing. Furthermore, relative to each neuron peak of activity (equal to 1), we also calculated the burst duration as the time interval between the first bin before and after the peak of activity whose value was higher and lower than (1 - B)*0.25 + B, respectively, where B is the mean baseline activity. Finally, one-way repeated measures sliding ANOVAs were used to verify, for each neuron, differences ($p<0.05$ uncorrected) between the compared conditions (e.g. object type). This analysis was performed in 500 ms epochs, slit forward in steps of 20 ms. The results of these analyses were plotted (relative to the center of each epoch) by calculating the percentage of significantly tuned neurons in each epoch within each neuronal population.

2.8 HEAT MAPS CONSTRUCTION

Heat maps have been built to show the temporal activation profile of individual neurons in selected populations. Each line represents the activity of a single unit averaged across trials. The color code represents the net normalized activity, computed as follows: for each neuron, a mean baseline value across the trials was computed (500 ms before object presentation), and then subtracted bin-by-bin for the entire task period. Activity was aligned to the object presentation and the movement onset. Suppressed responses were flipped according to single unit analysis results. Finally, the net activity was normalized to the absolute maximum bin value (in each individual cell) across the conditions. All final plots were performed using a bin size of 100 ms and steps of 20 ms.

2.9 CORRELATION ANALYSES

Correlation analyses were performed by means of a two-tailed Pearson's correlation test (Matlab), carried out on different variables, namely, the peak of activity, peak of activity timing, burst duration, and preference index associated with Go conditions of the execution and observation task. Each of these parameters was calculated, for each neuron, in a time window ranging from 0.5 s prior to movement onset to 0.8 s after this event in the case of action-related neurons, and in a time window ranging from object presentation to 0.8 s after this event in the case of object-related neurons. Each parameter, regardless of the reference time window, was calculated as follows.

Peak of activity. A mean value across all 36 trials (averaging the three objects) was computed in 20 ms bins. The highest value (Spk/s) within the reference time window was selected as peak of activity.

Peak of activity timing. The time bins corresponded to the peak of activity relative to the reference event of interest (object presentation or movement onset, in the case of object-related and action-related neurons, respectively) were selected as peak of activity timing.

Burst duration. We identified the first bin before (start) and after (end) the peak of activity corresponding to an activity value lower than 66% of the peak-activity value: the time lag between start and end of the discharge period including the peak of activity was selected as burst duration.

Object Preference Index. The preference index was calculated as defined by Moody and Zipser (Moody & Zipser, 1998) with the following Equation:

$$PI = \frac{n - \left(\frac{\sum r_i}{r_{pref}}\right)}{n - 1}$$

where n is the number of objects used, r_i is the activity associated to each object, and r_{pref} is the activity associated with the preferred object. The index can range from 0 (lack of selectivity) to 1 (response to only one object).

To check for possible differences in the distribution of the values associated to each factor between the tasks, we also performed a paired-samples t-test ($p<0.05$).

2.10 DECODING ANALYSES

The methodology employed for the decoding analysis was the same as the one previously described by Meyers (Meyers, 2013) and used in other studies (Zhang *et al.*, 2011; Rutishauser *et al.*, 2015; Kaminski *et al.*, 2017). Specifically, we assessed the decoding accuracy of a classifier trained to discriminate between 1) Go and No-Go trials, 2) the type of object used as target, and 3) the agent (monkey or experimenter).

For each neuron, data were first converted from raster format into binned format. Specifically, we created binned data that contained the average firing rate in 150-ms bins sampled at 50-ms intervals for each trial (data-point). We obtained a population of binned data characterized by a number of data points corresponding to the number of trials x conditions (i.e. 30 x 2= 60 data-points for Go/No-Go

decoding; 10 x 3= 30 data-points for object decoding during Go trials; 30 x 2 = 60 data-points for agent decoding during Go trials) in an N-dimensional space (where N is the total number of neurons considered for the analysis). Next, we randomly grouped all the available data points into a number of splits corresponding to the number of data points per condition, with each split containing a "pseudo-population", that is, a population of neurons that were partially recorded separately but treated as if they were recorded simultaneously. Before sending the data to the classifier, they were normalized by means of z-score conversion so that neurons with higher levels of activity did not dominate the decoding procedure. Subsequently, a pattern classifier was trained using all but one of the splits of the data and then tested on the remaining one: this procedure was repeated as many times as the number of splits (i.e., 30 times in the case of Go/No-Go decoding, 10 times in the case of object decoding; 30 times in the case of agent decoding), leaving out a different test split each time. To increase the robustness of the results, the overall decoding procedure was run 50 times with different data in the training and test splits, and the decoding accuracy from all these runs was then averaged. The decoding results were based on the use of a correlation-coefficient classifier. All the analyses were performed on data collected from the two monkeys, as well as on the data collected from each animal, separately.

Note that when this procedure is applied by training the classifier to decode a specific variable (i.e. the type of object) in one condition (i.e. execution task) and testing its performance in another condition (i.e. observation and extrapersonal task), the results of this cross-modal decoding provide information on the generalization of the population code across conditions.

Cross-decoding analysis has been performed also by 1) focusing on a single 1000-ms epoch (500 ms before and 500 ms after movement onset) of (self and other's) action execution to test whether and to what extent the population code could generalize across agents, and 2) focusing on a single 800-ms epoch of object presentation to self and other to test whether population code of object type could generalize across potential agents.

To assess whether the classification accuracy in the various analyses was above chance, we ran a permutation test in which we randomly shuffled the

attribution of the labels to the different trials, and then ran the full clutter-decoding experiment to obtain a null distribution to be compared with the accuracy of the real decoding: the p-value was found by assessing how many of the points in the null distribution were greater than those in the real decoding distribution and selecting only periods of at least 3 consecutive significant bins.

2.11 ANATOMICAL LOCALIZATION OF THE RECORDED REGION

To perform histological analysis aimed at identifying the exact location of the implanted probes, at the end of the experiments the monkey was anaesthetized with ketamine hydrochloride (15 mg/kg i.m.) followed by an intravenous lethal injection of pentobarbital sodium and perfused with saline, 4% paraformaldehyde, and 5% glycerol, prepared in 0.1M phosphate buffer, pH 7.4, through the left cardiac ventricle. The brain was subsequently removed from the skull, photographed and then frozen and cut into coronal sections of 60-μm thickness. The locations of the electrode tracks in the cortex were assessed under an optical microscope in Nissl-stained sections and then plotted and digitalized together with the outer and inner borders of the cerebral cortex using a computer-based charting system (for the details of the procedure see (Gerbella *et al.*, 2016). The cytoarchitectonic features of the recorded region were identified based on the criteria used to subdivide the mesial frontal areas by Matelli and coworkers (Matelli *et al.*, 1991; Belmalih *et al.*, 2007). To obtain monkey 3D volumetric brain reconstructions, containing the data regarding the location of the probe' traces, the data from individual sections were also imported into homemade software, allowing us also to cut the brain in slices of different planes and thickness. Finally, the schematic drawing of the implanted probes was superimposed on the exact location of the electrodes' traces on oblique re-sliced views of the 3D reconstructions in both hemispheres.

3. RESULTS

In both Experiments 1 and 2, neurons were recorded from the same five chronic arrays constituted by different configurations of linear multielectrode silicon probes, all implanted in area F6. Figure 6 shows the recorded regions in both hemispheres of M1 (Fig. 6a and b) after being reconstructed based on the histological identification of the probes' tracks from Nissl-stained coronal sections of the monkey's brain. The architectonic features of both recorded regions in M1 indicates that all probes were located within the anatomical borders of area F6. The reconstruction of the recording sites in M2 was performed with the same software and methodology but based on MRI slices of the monkey's brain.

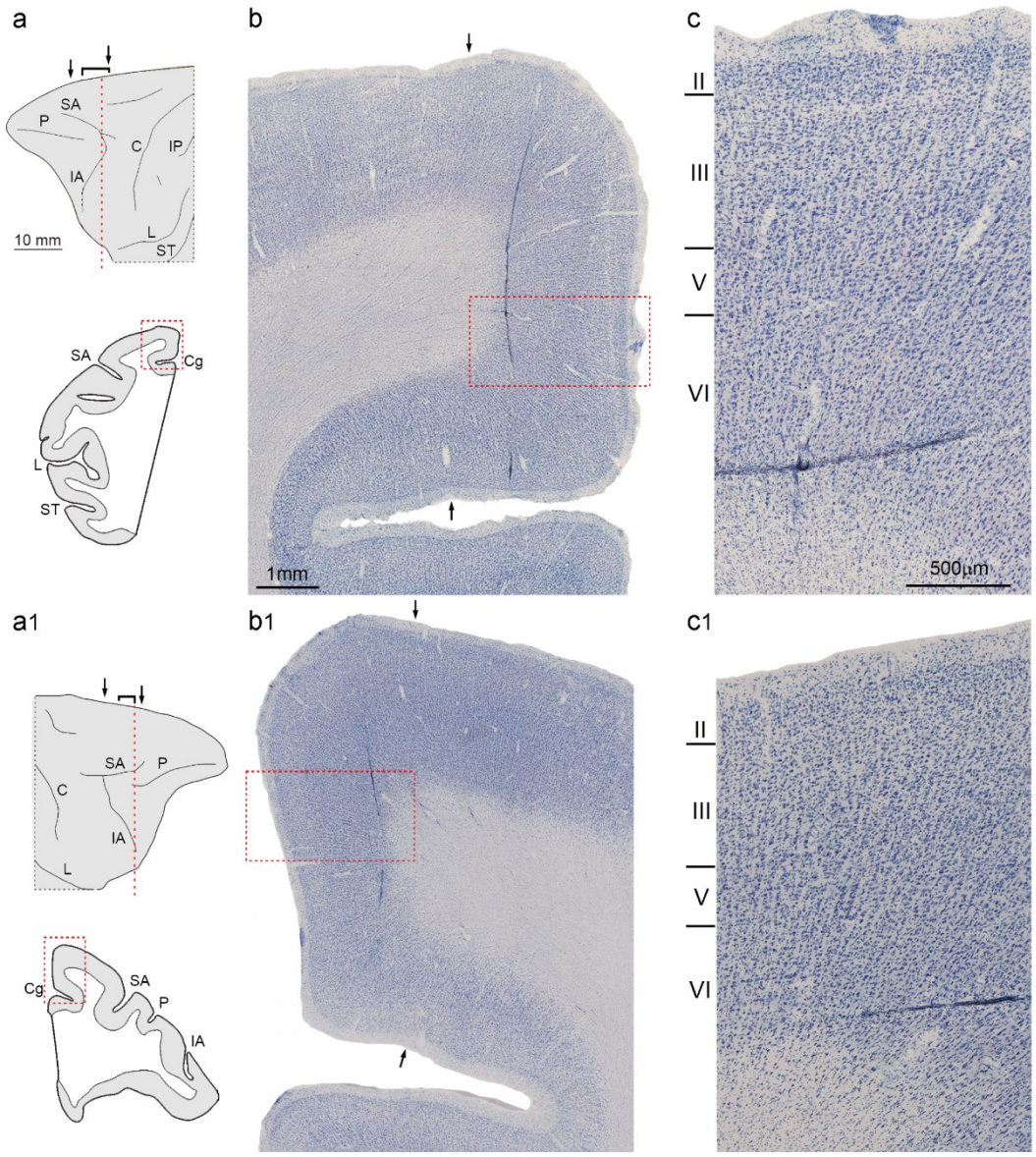

Figure 6. Histological identification of probes position and architectonic features of the recorded region. (a-a1) Dorsolateral view of the left (a) and right (a1) recorded hemispheres of M1. The square bracket on top of each brain indicate the rostro-caudal extension of the investigated sector, and the dashed red lines indicate the coronal sections (shown below) where the probe tracks in (b) and (b1) were identified. The black arrows indicate the histologically identified borders between area F6 and supplementary area F3 (posteriorly) and prefrontal area 8B (anteriorly). Dashed red boxes in each coronal section indicate the location of the photomicrograph showed in (b) and (b1). Scale bar in (a) applies also to (a1). (b-b1) Photomicrograph of Nissl stained sections in which it is possible to identify a probe track spanning the entire dorso-ventral extent of area F6. The dashed red boxes in (b) and (b1) indicate the cortical sector magnified in (c) and (c1). Scale bar in (b) applies also to (b1). Black arrows indicate the histological borders between area F6 and dorsal premotor area F7 (medially) and cingulate area 24 (ventrally). (c-c1) High magnification views of the cortical sector included in the red boxes of panels (b) and (b1) rotated by 90°. Note that the typical architectonic features of area F6 (Luppino et al. 1991) are evident, namely, a uniform layer III composed by small pyramids and a relatively prominent layer V populated by larger pyramids. Scale bar in (c) applies also to (c1).

Abbreviations as follow: C, central sulcus; Cg, cingulate sulcus; IA, inferior arcuate sulcus; L, Lateral sulcus; SA, superior arcuate sulcus; ST, superior temporal sulcus.

Figure 7 shows the exact location of the recorded regions on the three-dimensional reconstructions of both hemispheres of M1 (Figure 7a and b) and the right hemisphere of M2 (Figure 7c). Figure 7 also shows that visually triggered neurons (i.e., visual and visuomotor) and purely motor neurons were largely intermingled in both animals and were recorded even from the same contact in about 30% of the sites in which single unit activity was detected. Figure 7d shows the results of long-train intracortical microstimulation (ICMS) carried out in M2 (500 ms biphasic cathodic pulses at 300 Hz). In particular, we observed complex, multijoint and relatively slow movements involving the contralateral arm and the shoulder, often including the wrist and the hand (dark green circles in Figure 7d) and, in some cases, even synergic finger movements alone (light green circles). These findings are in line with previous ICMS studies on area F6 (Luppino *et al.*, 1991a), and indicate that neuronal activation in this region plays a role in the control of proximal as well as distal movements of the contralateral forelimb.

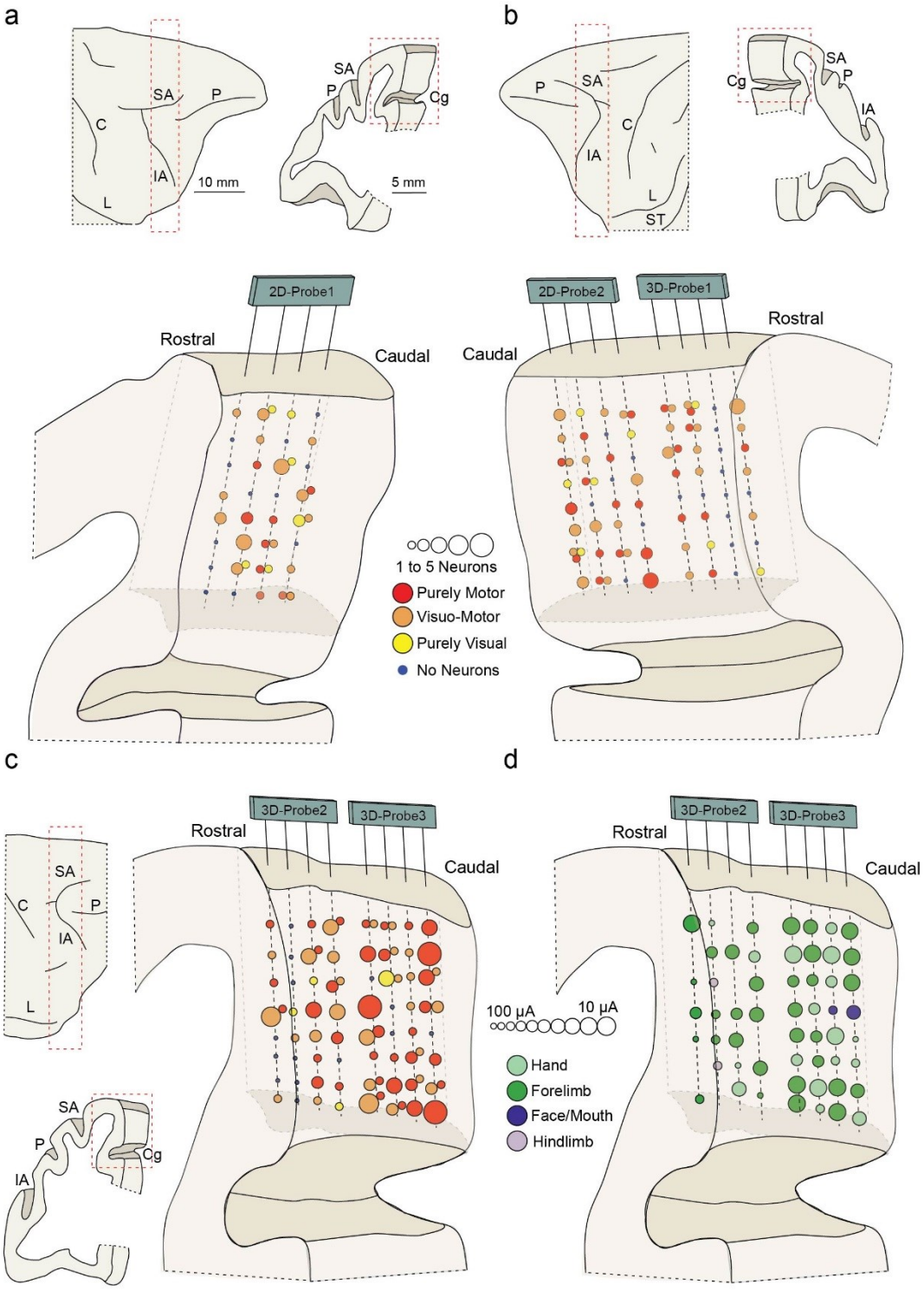

Figure 7. Reconstruction of the recorded regions and stimulation experiments. Anatomical reconstruction of the right (a) and left (b) hemispheres of M1, with superimposed probes' trajectory. Adjacent electrodes spaced by 300 µm are plotted as one line. (c) Anatomical reconstruction of the right hemisphere of M2. (d) Results of an ICMS mapping study carried out on M2 at the end of the recordings. Note that two sites on the most caudal part of the recorded region were associated to face-mouth movement, which is known to correspond to the functional border between areas F3 (caudally) and F6 (rostrally) (see *(Luppino et al., 1991a)*. The size of the circles corresponds to the current intensity threshold (see Materials and Methods). Scale bars in (a) applies also to (b) and (c). Abbreviations as in Figure 6.

3.1 EXPERIMENT 1

We recorded a total of 355 single neurons during the Execution task, of which 233 (65.6%) were classified as task related based on the statistical analysis of their response during the different conditions and epochs (see Materials and Methods). Among task-related neurons, 108 were purely motor, 103 were visuomotor and 22 were purely visual neurons. Example neurons are shown in Figure 8. Neurons classified as purely motor discharged only during reaching-grasping execution (Neuron 1), visuomotor neurons became active during both the object presentation epoch and reaching-grasping execution (Neuron 2), and purely visual neurons discharged only during object presentation (Neuron 3). Note that all these example neurons also showed differential activation depending on the target object. Extensive details on all the recorded neurons' motor and visual preferences for the target object are provided in Table 1, as well as in the following sections.

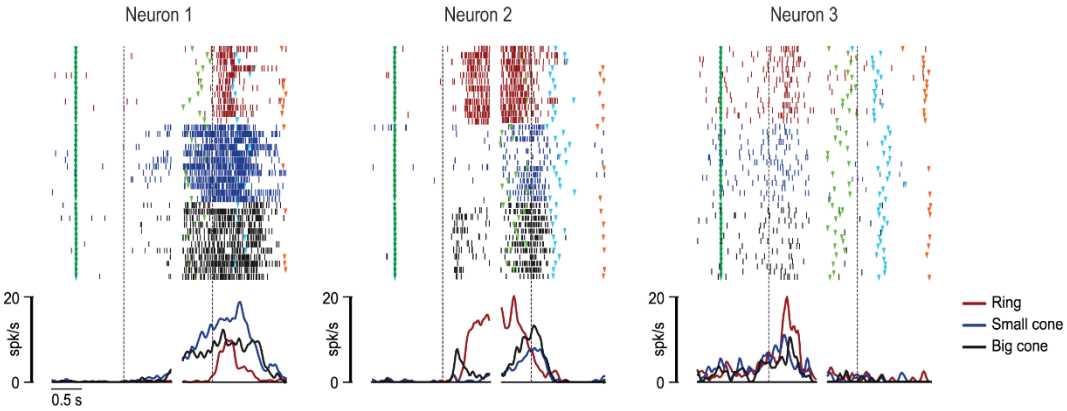

Figure 8. **Main single neurons categories example.** Examples of the three main types of neurons recorded during task execution. For each neuron rasters and spike density function are aligned (dashed lines) on object presentation (left part) and, after the gap, on the moment when the monkey's hand detached from the starting position (right part). Markers: dark green, cue sound onset (beginning of the trial); light green, end of the cue sound (go signal); light blue, object pulling onset; orange, end of the trial and reward delivery.

Neuron class	Ring	Small cone	Big cone	Two objects	Unselective	Total
Purely motor*	11	6	7	8	76	108
Visuomotor*	13	2	2	5	81	103
Purely visual*	5	0	0	1	16	22
Total	29	8	9	14	173	233

Table 1. Object preference of all the recorded neurons. * For purely motor neurons object preference was considered during reaching-grasping execution epochs, whereas for visuomotor and purely visual neurons, object preference was considered during the target presentation epoch.

Purely motor neurons

Most purely motor neurons (n=75, 69.4%) discharged similarly during reaching-grasping in the light and in the dark, although some showed a stronger discharge either in the light (n=23, 21.30 %) or in the dark (n=10, 9.3%). Among purely motor neurons, 32 (29.6%) discharged differently depending on the grasped object. Figure 9a shows examples of grip-selective F6 motor neurons tested during reaching-grasping in the light and in the dark. Neuron 1 is a typical example of a grip-selective neuron, which discharged more strongly when the monkey grasped the ring regardless of whether grasping was performed in the light or in the dark. Neuron 2 exhibited a preferential discharge for the big cone, but its activity was stronger during grasping in the light, whereas Neuron 3 showed the opposite modulation, being more strongly activated during grasping in the dark than in the light, with a preferential discharge for the big and small cones relative to the ring. It is clear from the neuron examples that the target selectivity of F6 purely motor neurons cannot be accounted for by vision of the object. This conclusion is also supported by population activity, which shows that both motor activity and object selectivity assessed during grasping in the light remained the same even during grasping in the dark (Figure 9b).

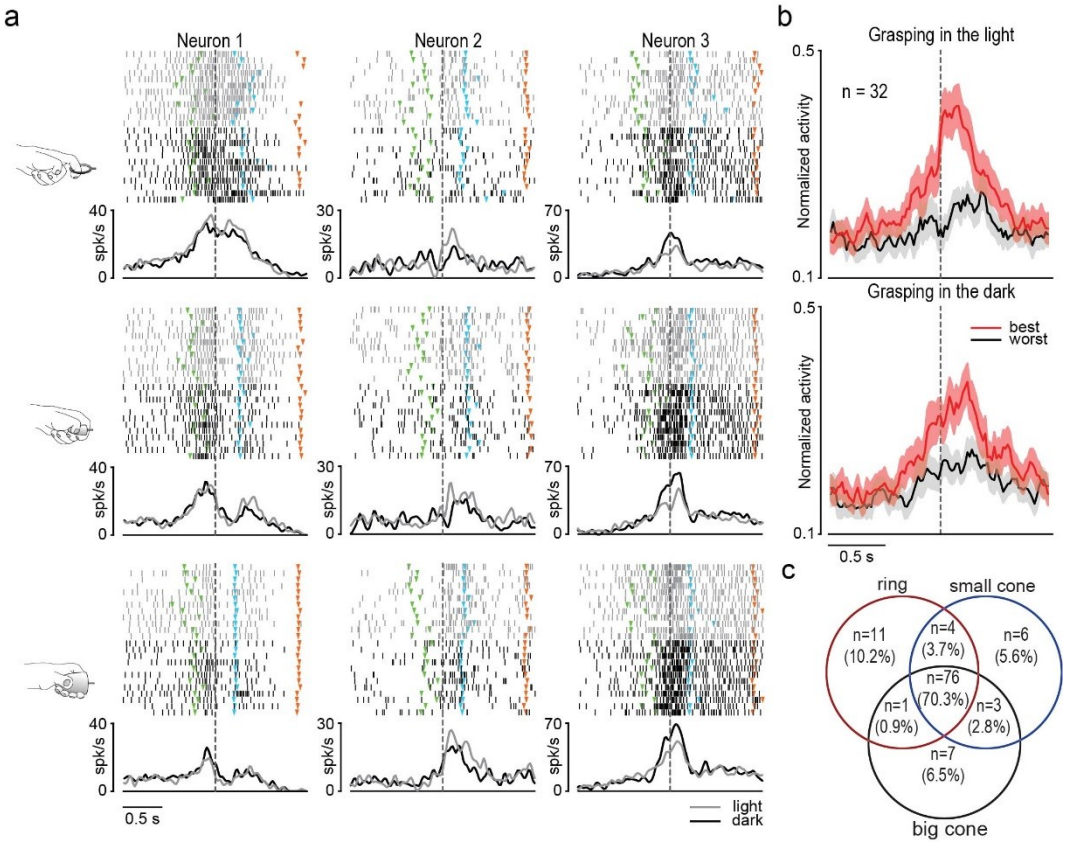

Figure 9. Functional properties of F6 purely motor neurons. (a) Examples of three F6 purely motor neurons showing selectivity for the target object. The image on the left of each line of the panel shows the type of grip employed by the monkey in that trials. Other conventions and markers as in Figure 8. (b) Population activity of purely motor neurons with object selectivity. As for single neuron examples, the activity is aligned to the movement onset, and shows the averaged population response to the preferred and non-preferred target established on the basis of each neurons response during grasping in the light. The coloured shaded area around each curve represents 1 standard error. By means of 2x3 repeated measures ANOVAs (factors: Object and Epoch) applied to each condition (light and dark), separately, we observed that this neuronal population responded and showed object selectivity during both pre-movement and reaching-grasping in the dark ($p<0.001$) as well as in the light ($p<0.001$). Furthermore, the population response to each object (best and worst) in the light was not significantly different from that to the same object grasped in the dark, neither during the pre-movement (Best $t=0.076$, $p= 0.94$; Worst $t=0.40$, $p= 0.69$) nor in the reaching-grasping (Best $t=2.01$, $p=0.052$; Worst $t=0.61$, $p=0.55$) epoch. (c) Number of purely motor neurons with selectivity for one or two of the target objects, or with no object selectivity.

Interestingly, neuronal preference for the three tested objects was substantially balanced: indeed, we did not observe any prevalence either in terms of the number of single neurons that showed a preference for a particular object ($\chi^2 =1.75$ $p=0.42$, Figure 9c) or in terms of the overall intensity of population activity during the grasping of each of the objects (Figure 10). Altogether, these findings

indicate that the object selectivity of purely motor neurons reliably reflects a motor preference for the type of grip.

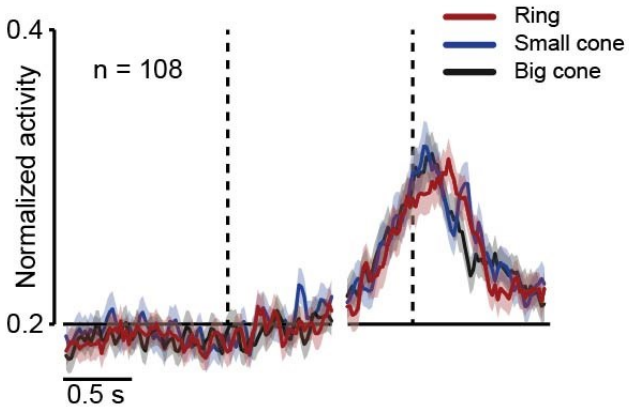

Figure 10. Population activity of all purely motor neurons during grasping each of the objects. The activity is aligned to the object presentation (dashed line on the left) and, after the gap, to the movement onset (dashed line on the right). The averaged population response has been computed taking into account each neurons response during grasping in the light for each object. The colored shaded area around each curve represents 1 standard error. By means of a 3x3 repeated measures ANOVA (factors: Object and Epoch), we observed that this neuronal population responded during both the pre-movement and reaching-grasping epoch relative to baseline ($p<0.001$), but it did not show any significant main or interaction effect for the factor "object".

Visually-triggered neurons

Among the 125 visually-triggered neurons (including both visual and visuomotor neurons), 28 (22.4%) showed object selectivity. Examples are provided in Figure 11a. Neuron 1 is a purely visual neuron that discharged selectively to the presentation of the ring during go trials but not during no-go trials. Note that in spite of its purely visual nature, the response of this neuron was highly context selective, because it encoded the ring only when it was the target of a forthcoming action. A similar selectivity was exhibited by Neuron 2, a visuomotor neuron with a clear-cut preference for the ring during go trials that stopped its firing after the onset of reaching. It is important to note that the discharge of both these neurons was more closely related to the object presentation than to the reaching-grasping epochs of the task. Although a few F6 visuomotor neurons (e.g. Neuron 3 in Figure 11a) exhibited a biphasic visual and motor response pattern, this latter activation profile was rare, and more importantly, it did not emerge from the population activity profile (Figure 11b).

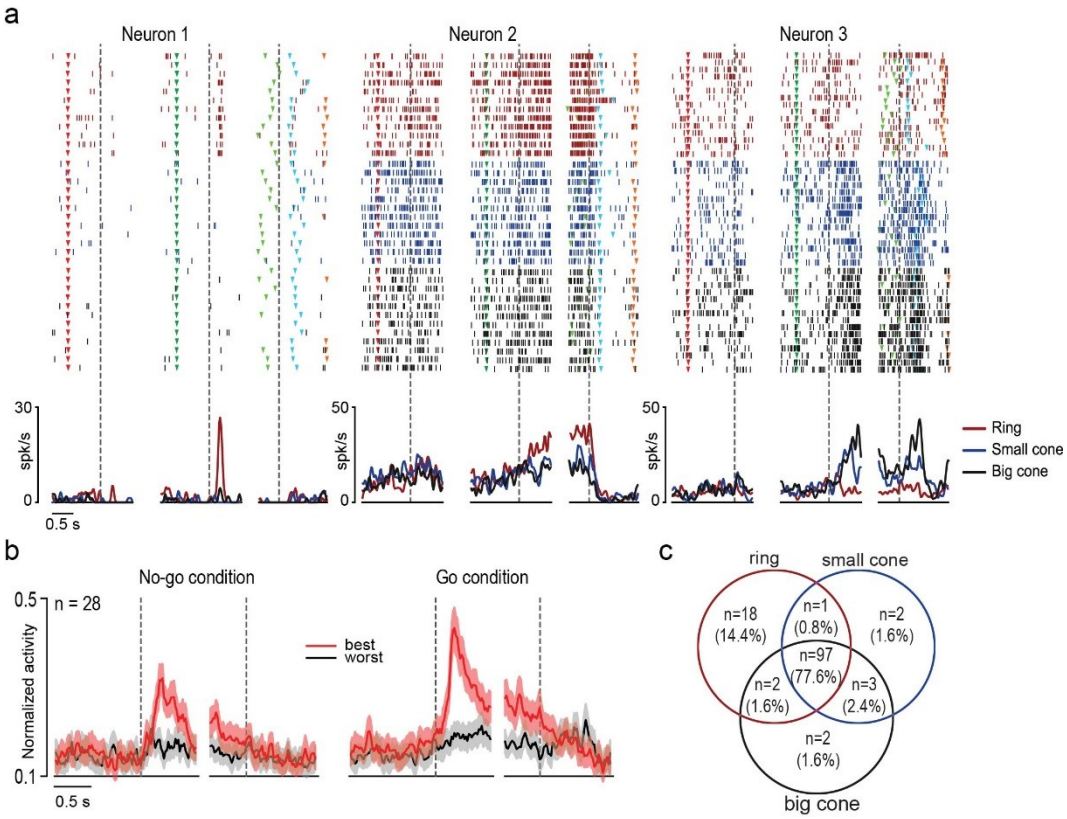

Figure 11. Functional properties of F6 visually-triggered neurons. (a) Examples of three F6 visually-triggered neurons showing visual selectivity for the target object. For each neuron rasters and spike density function have been aligned (dashed lines) to three different events, separated by a gap: 1) object presentation during no-go trials (on the left); 2) object presentation during go trials (on the center); 3) movement onset (on the right). Red triangular marker, no-go cue sound onset (beginning of the trial). Other conventions as in Figure 9. (b) Population activity of visually-triggered neurons with object selectivity. Best (red) and worst (grey) objects have been selected, for each neuron, based on the visual response during go-trials. In the no-go condition the activity is aligned to the object presentation (dashed line on the left) and, after the gap, to the no-go signal (dashed line on the right). In the go condition the activity is aligned to the object presentation (dashed line on the left) and, after the gap, to the movement onset (dashed line on the right). The population responses to object presentation during the go and no-go conditions have been analyzed separately by means of a 2x2 repeated measures ANOVA (factors: Object and Epoch). In both conditions there was a stronger visual presentation response for the best relative to the worst object ($p<0.001$), and the population response to this latter did not even reach significance during the no-go condition ($p=0.18$). Furthermore, the population response to the presentation of the best object was stronger when it occurred during go relative to no-go trials ($t=4.77$, $p<0.001$). Another 2x3 repeated measures ANOVA (factors: Object and Epoch) has been performed on the movement-related population activity, as well as on the population response aligned to the no-go signal. Interestingly, we found a significant response only for the best object relative to baseline during the pre-movement epoch ($p<0.001$) as well as during the epoch preceding the no-go signal ($p<0.001$), but not during the reaching-grasping epoch. Furthermore, the population activity preceding movement onset and the no-go signal did not differ significantly from each other ($t=1.85$, $p=0.075$). (c) Number of visually-triggered neurons with visual selectivity for one or two of the target objects, or with no object selectivity.

This phenomenon did not depend on the inclusion of purely visual neurons (6 out of 28), because it was present even when only visuomotor neurons were considered (Figure 12). These findings demonstrate that area F6 neurons can play a role in the visuomotor processing of objects, but their activation dynamic seems to be strikingly different from that of visuomotor neurons described in other brain regions (for a review see (Maranesi *et al.*, 2014a) , particularly area F5 (Murata *et al.*, 1997; Raos *et al.*, 2006; Bonini *et al.*, 2014c); for a direct comparison see the following section).

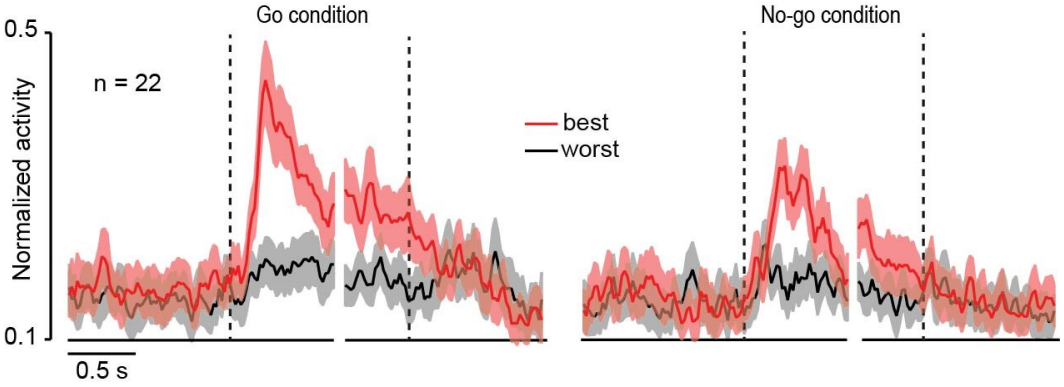

Figure 12. Population activity of visuomotor neurons with object selectivity. Population responses have been computed for the best (red) and worst (grey) objects identified, for each neuron, based on the visual response during go-trials. In the go condition the activity is aligned to the object presentation (dashed line on the left) and, after the gap, to the movement onset (dashed line on the right). In the no-go condition the activity is aligned to the object presentation (dashed line on the left) and, after the gap, to the no-go signal (dashed line on the right). The population responses to object presentation during the go and no-go conditions have been analyzed separately by means of 2x2 repeated measures ANOVAs (factors: Object and Epoch). In both conditions there was a stronger visual presentation response for the best relative to the worst object ($p<0.001$), and this latter did not even reach significance during the no-go condition ($p=0.18$). Furthermore, the population response to the presentation of the best object was stronger when it occurred during go relative to no-go trials ($t=3.58$, $p=0.026$). Another 2x3 repeated measures ANOVA (factors: Object and Epoch) has been performed on the movement-related population activity, as well as on the population response aligned to the no-go signal. Interestingly, we found a significant response only for the best object relative to baseline during the pre-movement epoch ($p<0.001$) as well as during the epoch preceding the no-go signal ($p<0.001$), but not during the reaching-grasping epoch. Furthermore, the population activity preceding movement onset and the no-go signal did not differ significantly from each other ($t=1.78$, $p=0.088$).

Another important finding is that object visual selectivity displayed by F6 neuronal population during go trials was also present during no-go trials, even though the discharge intensity was significantly reduced (Figure 11b). This suggests that visually triggered F6 neurons underlie visuomotor associations between

observed objects and the potential motor actions that can be performed on them. An interesting observation supporting this hypothesis is that, in contrast to the balanced motor selectivity for the different objects of purely motor neurons (see above), visually triggered neurons exhibited a preferential selectivity for the ring. This was evident both in terms of percentage of single neurons ($\chi 2 = 23.28$ $p<0.001$, Figure 11c) and in terms of intensity of the overall population response during visual presentation of the ring relative to the other objects (Figure 13). This finding may be due to the well-established role of F6 in forming new arbitrarily learned visuomotor associations (Nakamura *et al.*, 1998). Indeed, whereas the small and big cones were spontaneously grasped with a precision and power grip, respectively, monkeys would naturally grasp a small ring like the one used in this study by means of a side grip with 90° wrist rotation (personal observations) rather than by inserting just the index finger in it (hook grip). This latter grip type was achieved through a specific training, which may explain its visual overrepresentation.

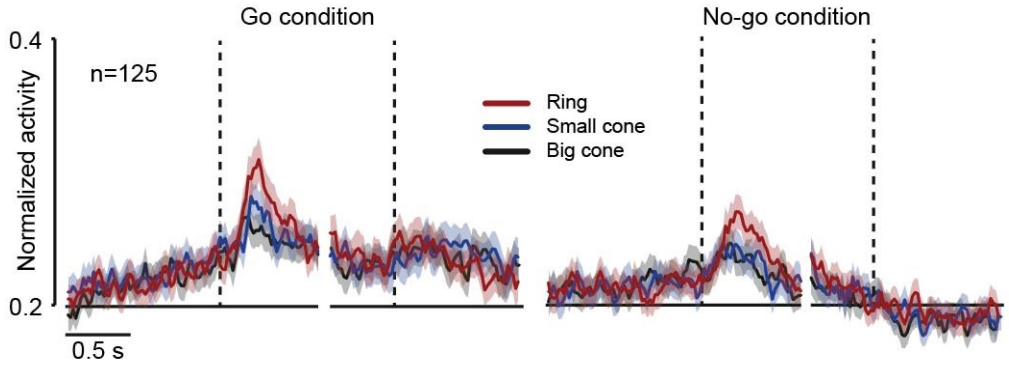

Figure 13. Population response of all visually-triggered neurons related to each of the tested objects. The population activity has been computed including both neurons with excitatory and neurons with inhibitory response. Conventions as in Figure 10. The population responses to object presentation during the go and no-go conditions have been analyzed separately by means of a 3x2 repeated measures ANOVAs (factors: Object and Epoch). In both conditions there was a stronger visual presentation response for all objects relative to the baseline ($p<0.001$). Interestingly, the response associated to the presentation of the ring during go-trials was stronger than that to both the small ($p=0.034$) and big ($p<0.001$) objects. Similar results have been obtained concerning object selectivity during no-go trials (ring vs. small, $p = 0.0057$; ring vs. big, $p<0.001$), although the response to the visual presentation of the ring was stronger during go relative to no-go trials ($t=3.54$, $p<0.001$). No significant differences were observed between small and big objects in both conditions. A 3x3 repeated measures ANOVA (factors: Object and Epoch) has been performed on the motor-related population activity, as well as on the population response aligned to the no-go signal. Interestingly, it revealed no significant difference for pre-movement and reaching-grasping epochs relative to the baseline during go trials ($p=0.81$), but a significant suppression during the epoch following the no-go signal relative to the baseline ($p<0.001$).

In order to better understand the functional relevance of F6 neurons in object visual processing we also employed a test previously used to characterize the activity of F5 visuomotor neurons (Bonini *et al.*, 2014b). In this test, carried out on the neurons recorded from M2 and from the left hemisphere of M1, a transparent plastic barrier was interposed between the monkey's hand and the target during trials cued with the high tone (go-cue). Note that the monkey was not instructed to refrain from acting (as during no-go trials), but the barrier actually prevented it from reaching and grasping the presented object. An example neuron tested in this condition is shown in Figure 14a. It is evident that this neuron, which discharged more strongly during go trials relative to no-go trials, did also respond during the barrier test, but with a response pattern more closely resembling the one displayed during no-go rather than go trials, even if the auditory cue was the high tone (go cue). A similar effect was evidenced by the population activity: indeed, the population response was stronger and showed the maximal selectivity during go trials relative to no-go trials, in line with single-neuron behavior, whereas during the barrier test the discharge intensity was similar to that during no-go trials but completely lacked object selectivity (see Figure 14b). Altogether, these findings indicate that object-selective visual responses of F6 neurons are strongly modulated by the contextual setting: indeed, their selectivity depends mostly on the monkey's intention and possibility to act on the object.

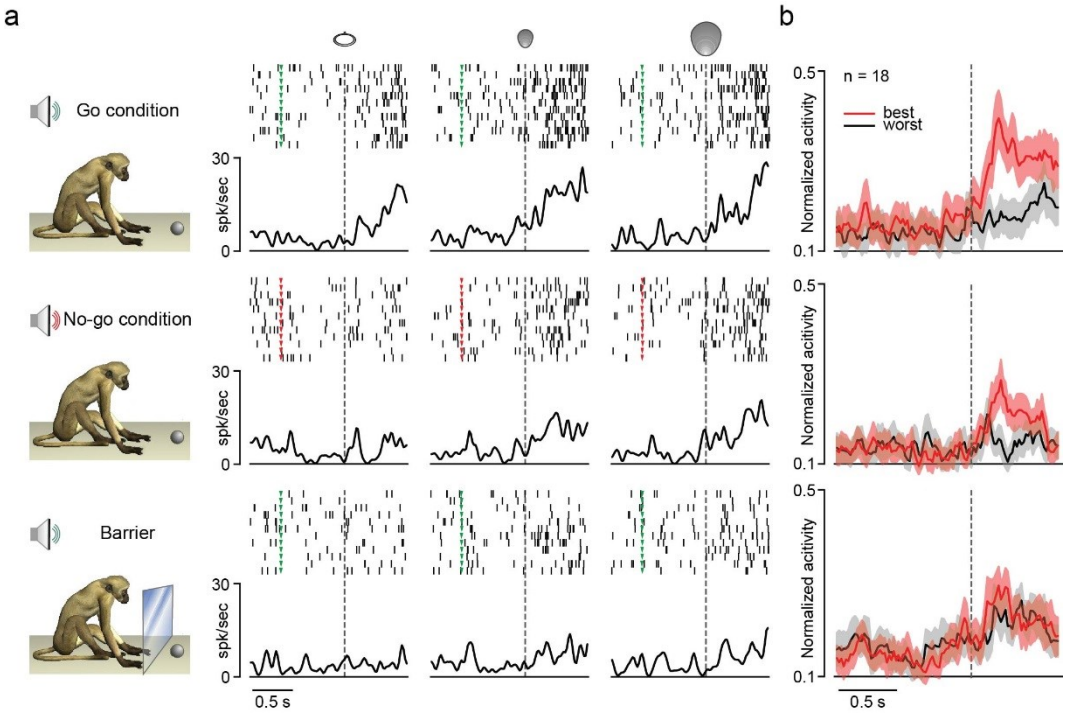

Figure 14. Visual responses of F6 neurons to object presentation in different contexts. (a) Example of an F6 visually-triggered neuron showing visual selectivity for the small and the big cone and reduced response and selectivity when tested with a plastic barrier interposed between monkey's hand and the target. Conventions as in Figure 9. (b) Population activity of all F6 visually-triggered neurons tested in the three conditions. The population responses to object presentation have been analyzed separately by means of 2x2 repeated measures ANOVAs (factors: Object and Epoch). The visual presentation response was stronger for the best relative to the worst object during both go and no-go conditions ($p<0.001$ for both post-hoc comparisons), but not during the barrier test ($p=0.32$). Furthermore, the population response to the presentation of the best object was stronger when it occurred during go relative to no-go trials ($t= 3.09$, $p<0.001$), while it was not different between no-go trials and those during the barrier test ($t=0.015$, $p=0.99$).

Neuronal properties and dynamics in mesial (F6) and ventral (F5) premotor cortex

According to a widely accepted view, the mesial premotor cortex encodes triggering signals for starting and sequencing self-initiated actions, whose details, such as reach direction and grip type, are processed by dorsolateral premotor areas by means of parieto-premotor interactions (Rizzolatti & Luppino, 2001; Cisek & Kalaska, 2010; Kaas & Stepniewska, 2016a). In order to investigate the relative contribution of mesial and ventral premotor areas in reaching-grasping actions, we compared the response properties of neurons recorded from area F6 in this study with those previously recorded from area F5 with the same behavioral paradigm and in the same animals (Bonini *et al.*, 2014b; Maranesi *et al.*, 2015).

Figure 15 a-d shows the response dynamic of all area F6 recorded neurons with an excitatory response pattern and classified as visuomotor (Figure 15a and b) or purely motor (Figure 15c and d) neurons. Figure 15e-h shows the response dynamic of neuronal populations with the same features recorded from area F5. For both areas, single-neuron and population activity is aligned to the visual presentation of the preferred target (left part of each panel) as well as to the onset of the reaching-grasping movement (right part). Several interesting differences emerge between the two areas. First, area F6 neurons are characterized by relatively shorter bursts of activity as compared with those of F5 (see Materials and Methods), and this finding is evident and consistent for both visuomotor (Figure 15a and 15e) and purely motor (Figure 15b and 15g) neurons considered separately (Figure 16a and 16b).

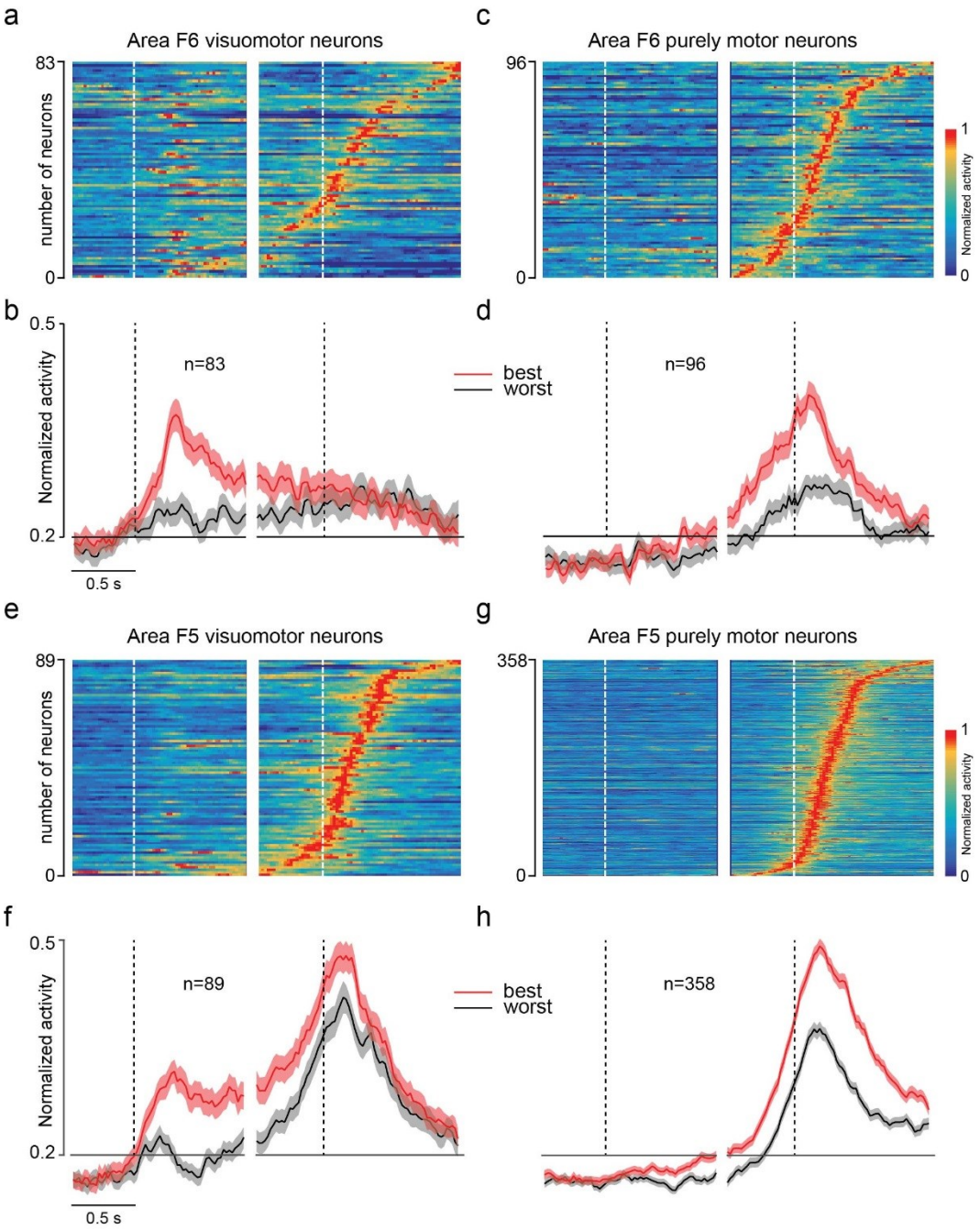

Figure 15. Comparison of neuronal dynamic and object selectivity between F5 and F6 visuomotor and purely motor neurons. Normalized activity of (a) visuomotor and (c) purely motor neurons of area F6 ordered based on the timing of their peak of motor activity (earliest on bottom). Each row represents a single neuron. White dashed lines represent the different alignment events: first (on the left, before the gap) object presentation, second (on the right, after the gap) hand movement onset. (b and d) Averaged population activity of the visuomotor (b) and purely motor (d) neurons of area F6 shown in (a) and (c). Black dashed lines corresponds to the same alignment events described in (a) and (c). Other conventions as in Figure 11b. (e-h) Normalized single neuron (e and g) and population (f and h) activity of visuomotor and purely motor neurons recorded from area F5 of the same animals and with the same task. All conventions as in (a-d).

Second, in area F6, both of these types of neurons peak earlier than cells of the same type recorded in area F5, where, in turn, most of the neurons display their motor-activity peak in a restricted time window centered on the hand-object interaction (Figure 16). Third, it is evident that many more neurons in F6 (Figure 15a and c) than in F5 (Figure 15e and g) alternate phases of increase and decrease in their activity: together with the above-mentioned features, this may explain the extremely different population response observed in the two areas (Figure 15b, d, f and h). Indeed, the neuronal population of F6 visuomotor neurons is characterized by a vigorous activation during the visual presentation of the target, where it also exhibits remarkable object selectivity, but it does not display any subsequent motor-related activation peak (Figure 15b). In contrast, visuomotor neurons of area F5 display the typical visual-to-motor activation and selectivity pattern highlighted by several previous studies (Murata *et al.*, 1997; Raos *et al.*, 2006; Bonini *et al.*, 2014b; Schaffelhofer *et al.*, 2015), in which the motor-related discharge is even stronger than the visual one (Figure 15f). The population dynamic of purely motor neurons is, instead, remarkably similar in the two areas (Figure 15d and h).

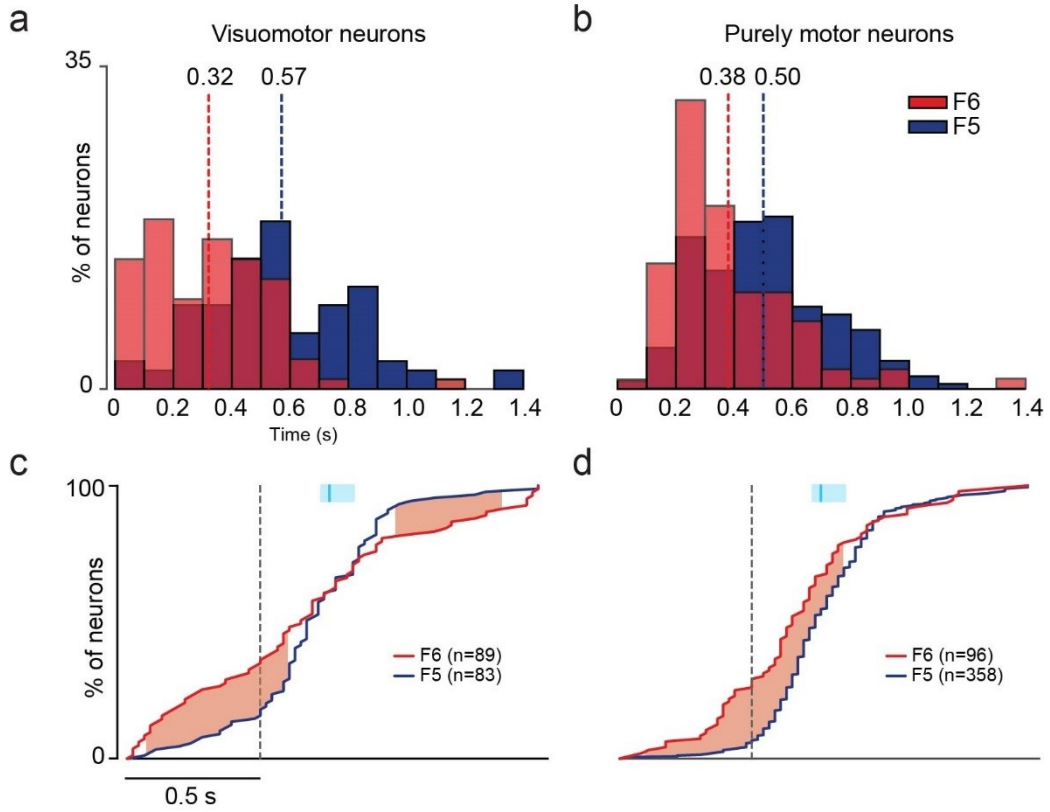

Figure 16. Comparison of area F6 and F5 neurons firing properties. (A and B) Distribution of burst duration for (A) visuomotor and (B) purely motor neurons of F6 (red) and F5 (blue). In both classes of neurons there was a prevalence of shorter bursts in F6 relative to F5 (visuomotor neurons, $t=6.8$ $p<0.001$; purely motor neurons $t=4.8$ $p<0.001$). (C and D) Cumulative distribution of activity peak timings of (C) visuomotor and (D) purely motor neurons in both areas F6 (red) and F5 (blue) relative to the movement onset. The red shaded areas represent the time interval in which the proportions of F6 and F5 neurons were significantly different from each other (χ^2 test, $p<0.05$). Light-blue bars on top of panel (C) and (D) represent the median times of object-pulling onset, and the shaded areas around each marker represent the 25th and 75th percentile times of other events of the same type.

Further important differences emerged in terms of overall object selectivity. We showed that in area F6 there is a prevalence of visual selectivity for the ring (Figure 11c and Figure 13) and no significant motor bias for any of the three tested objects (Figure 9c and Figure 10). This finding is also clearly evidenced in Figure 17a: a visual bias for the ring is exhibited by F6 visuomotor neurons from the visual presentation of the object until movement onset, whereas no significant bias emerged among purely motor neurons (Figure 17b). In contrast, in area F5 we observed that both visuomotor (Figure 17c) and purely motor (Figure 17d) neurons displayed a strong motor bias in favor of the small cone (i.e., precision grip), including a preparatory component that is more evident in purely motor neurons.

Altogether, these findings suggest that while in F6 there is a prevalence of visuo-preparatory selectivity for the object that was subject to the more intensive visuomotor training (the ring, to be grasped with an hook grip), in F5 prevails the motor representation of the most natural and widespread types of grip (Macfarlane & Graziano, 2009), which are typically used by monkeys to grasp and manipulate objects with no need of any explicit training.

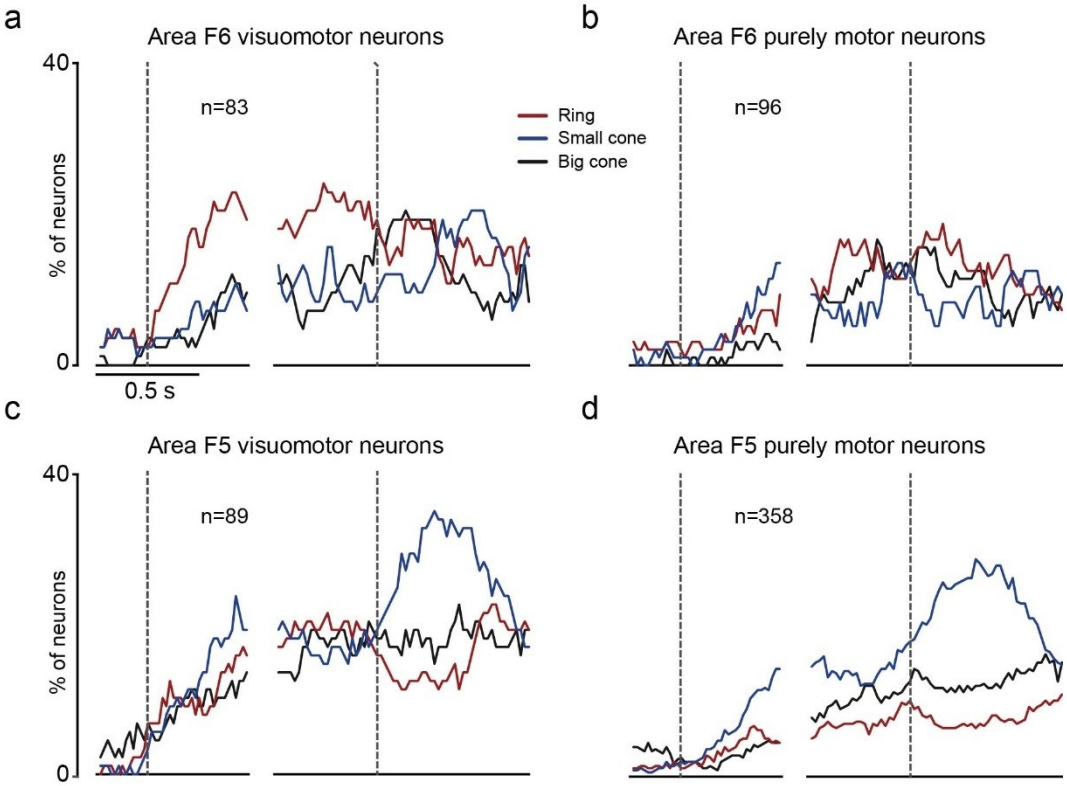

Figure 17. Comparison of object visual and motor selectivity of F5 and F6 neurons. (a-d) Each plot shows the percentage of neurons of each category and in each area exhibiting selectivity for one of the three tested objects during go-trials in the light (sliding 1-way repeated measures ANOVA, factor: Object, $p<0.05$ uncorrected – see Materials and Methods).

3.2 EXPERIMENT 2

In Experiment 2 we tested F6 neurons while monkeys not only Execute, but also Observed, the task performed by an experimenter within their peripersonal space, from a subjective viewpoint. This allowed us to test visual presentation responses when the same objects in the same context were visually presented to the animals as possible target for another agent.

Monkeys react differently to the same cue depending on task context

Both animals, depending on the task context, responded differently to the auditory Go cue (Figure 18a). They typically reacted to the end of the Go auditory cue (Go-signal) by detaching the hand from the starting position and reaching for the target in the execution task but not in the observation task. Furthermore, during the observation tasks, the location of the target within the peripersonal or extrapersonal space, and hence the monkey's possibility to interact with it, did not affect the probability of incorrectly detaching the hand from the starting position.

The analysis of errors suggests that monkeys discriminated the behavioral meaning of the auditory cues depending on task context. However, they could still exhibit a subtler preparatory activity that does not result into an overt behavioral error but could nonetheless affect muscles activity. To resolve this question, we recorded electromyographic (EMG) activity by placing surface EMG electrodes over a proximal and a distal muscle of the monkeys' forelimb during all task conditions, after the end of the neuronal recording sessions. We only observed significant muscle activation ($p<10^{-10}$ for both monkeys) following the Go-signal in the execution task (Figure 18b). Altogether, these findings indicate that both monkeys discriminate whether the cues were addressed to themselves or to the experimenter, depending on the task context.

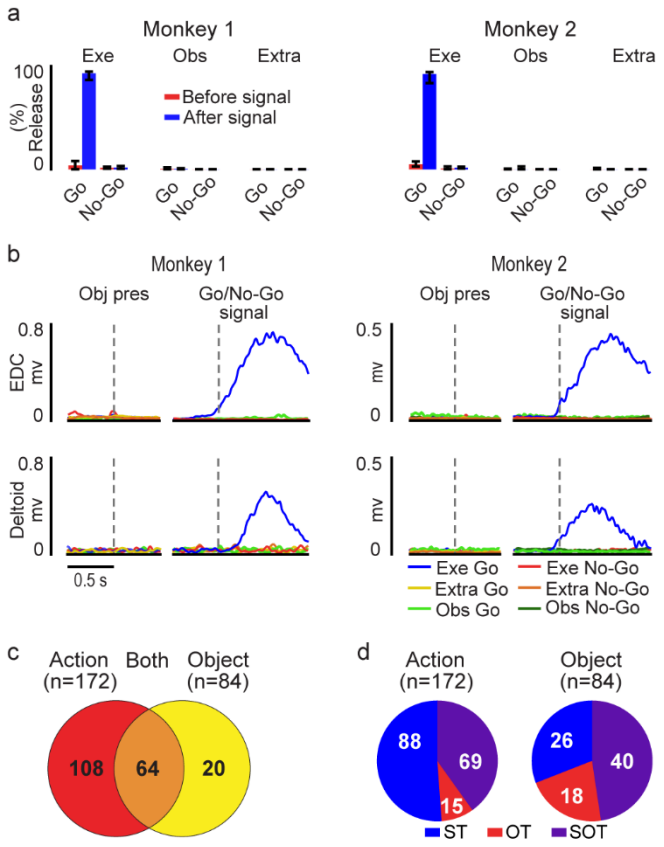

Figure 18. Behavioral data, and main neuronal categories. (a) Median percentage (across sessions, 5 for M1 and 9 for M2) of events in which the monkey releases the manipulandum in the period before (red) and after (blue) the Go and No-Go signal in the execution (Exe), observation (Obs) and extrapersonal (Extra) tasks. Error bars indicate the 5th and 95th percentile. (b) EMG temporal activation profile of the distal (Extensor Digitorum Communis, EDC) and proximal (Deltoid) muscles recorded in the two monkeys during different task conditions aligned (dashed lines) on object presentation (Obj pres) and, after the gap, on the Go/No-Go signal. (c) Number of task related neurons classified as action-related, object-related, or both. (d) Agent selectivity of action- and object-related neurons (ST, self-type neurons; OT, other-type neurons; SOT, self-and-other type neurons).

Agent-based representation of manual actions and graspable objects at the single neuron level

We recorded the activity of 306 single neurons during the execution and observation task, out of which 192 were classified as task related because they encoded executed and/or observed action, object, or both (see Methods).

A set of neurons responded only during execution and/or observation of the action (n=108), others only to the visual presentation of the object during the execution and/or the observation task (n=20), and another set (n=64) responded

during both object presentation and action execution/observation (Figure 18c). The three sets of neurons were substantially intermingled along the rostro-caudal extent of the recorded regions in both monkeys (Figure 19). All the neurons responding at least during action execution and/or observation were classified as action-related (n=172) and all those discharging at least to object presentation were classified as object-related (n=84). Based on this classification, we first asked whether and to what extent F6 neuronal representations of object and action differed depending on the agent (i.e. monkey or experimenter, see Methods): we found evidence of agent selectivity in both (Figure 18d).

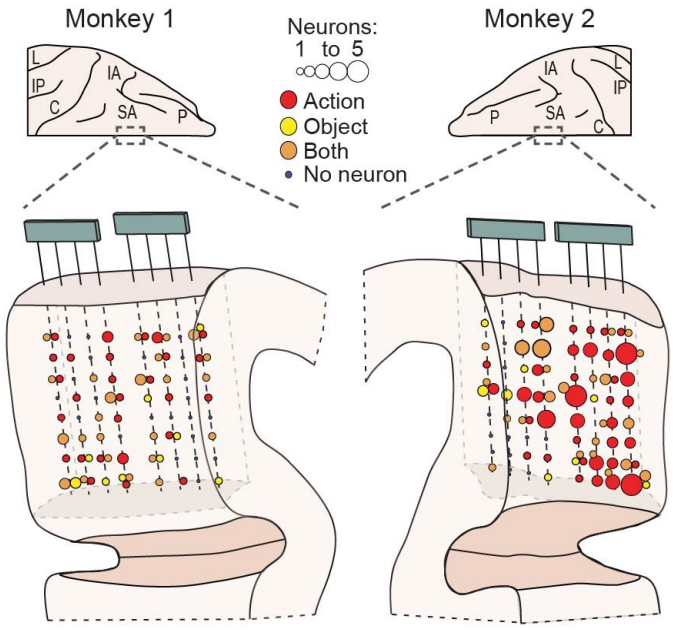

Figure 19. Distribution and localization of Action- and Object-related neurons. Reconstruction of the anatomical distribution of task-related neurons in the investigated regions for Action (red), Object (yellow) and neurons responsive for both (orange). L, lateral sulcus; IP, intraparietal sulcus; C, central sulcus; IA, inferior arcuate sulcus; SA, superior arcuate sulcus; P, principal sulcus.

Self-biased agent-based representation of reaching- grasping actions

Our reaching-grasping task allowed us to distinguish three main activation patterns of F6 action-related neuron (Figure 18d), which we defined by adopting the same classification criteria proposed by a previous study on arm reaching actions (Yoshida *et al.*, 2011). The majority of action-related neurons (n=88, 51%) became active only during monkey's own action (self-type neurons, ST, Figure 20a, b),

some (n=15, 9%) only during experimenter's action (other-type neurons, OT, Figure 20c, d), and another set (n=69, 40%) during both monkey's and experimenter's action (self-and-other type neurons, SOT, Figure 20 e, f). These latter neurons exhibited the same type of response pattern that characterizes classical mirror neurons, originally recorded from the monkey ventral premotor cortex (Gallese *et al.*, 1996; Rizzolatti *et al.*, 1996) and deemed to provide a shared neural substrate for the representation of self- and others' action.

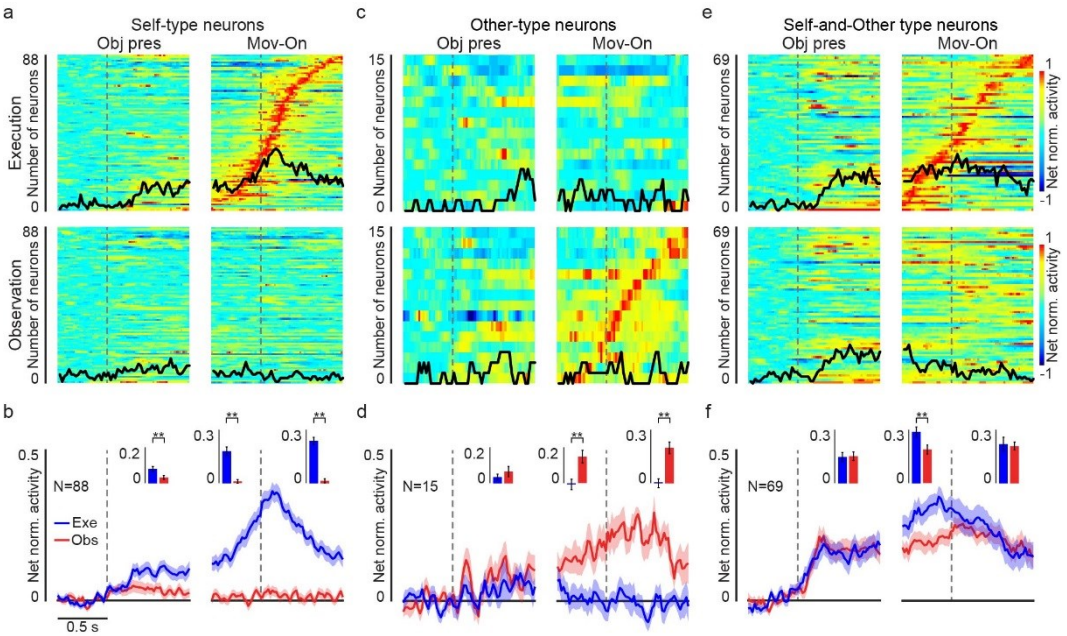

Figure 20. Single neuron and population activity of self, other, and self-and-other type action-related neurons. (a, c and e) Heat map plots of the temporal activation profile of single unit net normalized activity for ST (a), OT (c), and SOT (e) action-related neurons. Each of these sets of neurons is aligned first to the object presentation (vertical dashed line in the left panel), and then (after the gap) to the movement onset (signaled by the detachment of the hand from the starting position) during the execution (top row) and observation (bottom row) task. Neurons are ordered based on the timing of their peak of activity in the movement period of the execution task, in case of ST and SOT neurons (panels a and e), or of the observation task, in case of OT neurons (panel c), with the earliest on the bottom for all plots. The response to the three objects is averaged. The black line superimposed to each heat map plot indicates the number of neurons (same scale on the left) in each population showing selectivity for the type of object (sliding ANOVA $p<0.05$, uncorrected). (b, d and f) Time course and intensity of the mean net normalized population activity for the three sets of neurons shown in the correspondent panels above, during the execution (blue) and observation (red) task. The shading around each line indicates 1 standard error. Histograms in the insets of each panel represent the mean activity in each epoch for the two compared conditions. Paired-samples t-tests * $p < 0.05$, ** $p<0.01$.

Examples of two SOT action-related neurons are shown in Figure 21a: the monkey actively grasped the target object in the execution task whereas it remained still during the observation task, but these neurons encoded both self- and other-action, although with some differences between the two conditions (e.g. Neuron 2). To quantitatively assess the relationship between self- and other-action coding, we statistically analyzed parameters of action-related neuronal activity in the two contexts (execution and observation). We found that the peaks of activity (Figure 21b) and their timing (Figure 21c), the bursts' duration (Figure 21d) and the neural preference for objects (Figure 21e) were significantly correlated between the two tasks, although both the peak of activity and the neural preference for objects were greater during the execution relative to the observation task (Figure 21d, f).

To further clarify whether and to what extent SOT action-related neurons provide a shared code for self- and other-action, we performed a cross-modal decoding analysis (see Methods) aimed at discriminating the target objects during both the execution and the observation task using a classifier (Meyers, 2013) trained on the activity recorded during either action execution (Figure 21f, Train on Exe) or action observation (Figure 21f, Train on Obs). The results did not show evidence of cross-modal decoding: indeed, object decoding accuracy was above chance level only when training and testing data for the decoder came from task execution, suggesting that this effect is mostly due to a somato-motor signal related to the grip type rather than to a visuomotor signal related to object features. This finding indicates that SOT neurons, in spite of their activation during both action execution and observation, convey more detailed information about one's own than others' action and can therefore contribute to self-other distinction. To more directly assess this hypothesis, we trained the classifier to distinguish self- from other-action (regardless of the target) based on the activity of SOT neurons recorded during own-action execution and other-action observation: by testing the decoding performance (see Methods), we found that SOT neurons' activity makes it possible to decode the agent (monkey or experimenter) with high accuracy even prior to movement onset (Figure 21g), likely because of the self-bias that is also evident in SOT action-related neurons' population activity (Figure 20e, f).

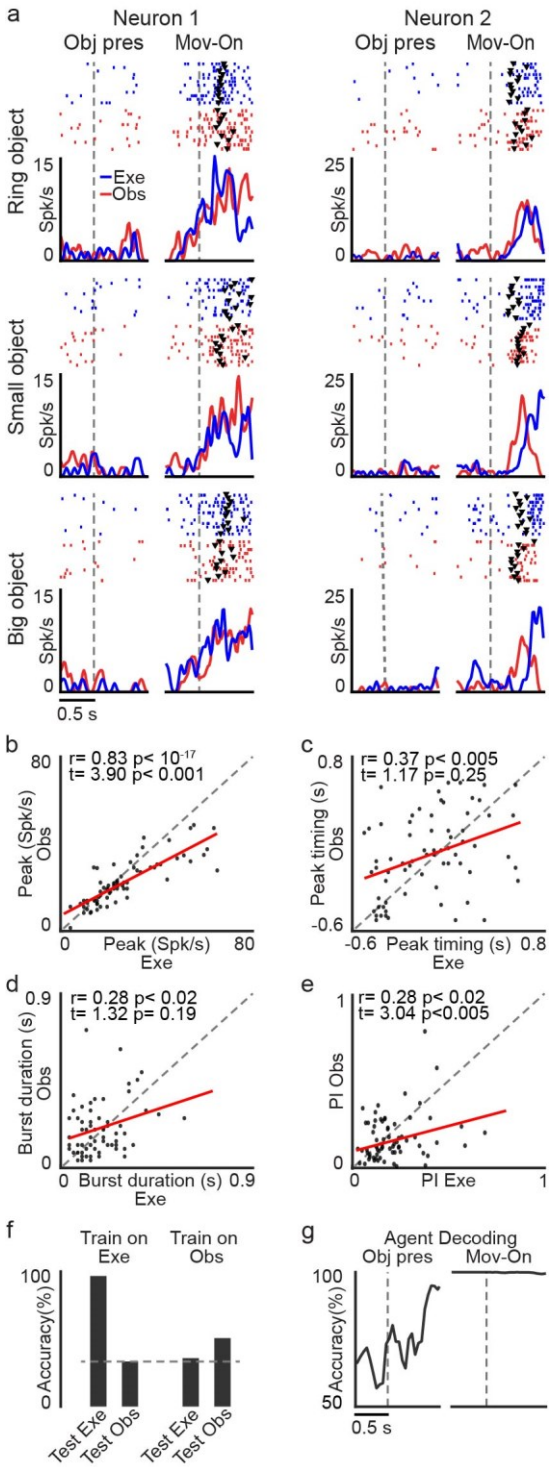

Figure 21. Relationship between SOT action-related neurons response during own action execution and other's action observation. (a) Single neuron response (raster and line plot) during task execution (Exe, blue) and observation (Obs, red) aligned (vertical dashed lines) on object presentation (Obj pres) and (after the gap) movement onset (Mov-on) with the three different objects as targets. Small black triangular markers in the rastergrams indicate the timing of object-pulling onset in each trial. (b) Correlation plot of peak activity (in spikes/second) of the same cells (n=69) during action execution and observation, in the -0.5/+0.8 second interval relative to movement onset. (c) Correlation plot of peak activity timing of the same cells during execution and observation (same period of B). (D) Correlation plot of burst duration (see Methods) of the same cells during action execution and observation. (E) Correlation plot of the object preference index (PI, see Methods) calculated for the same cells on the responses during action execution and observation. (F) Accuracy in the classification of the target object (ring, small and big cones) during execution and observation

trials based on a training of the classifier carried out with SOT action-related neurons activity collected during either one of the two tasks. (G) Time course of the agent decoding accuracy based on SOT action-related neurons activity collected during task execution and observation.

Agent-based representation of graspable objects

The target presentation response of object-related neurons could show agent selectivity as well (Figure 18d). Some object-related neurons (n=26, 31%) became active only when the visually presented object was the target of monkey's own action (self-type neurons, ST, Figure 22a, b), 18 (21%) only when the object was the target of the experimenter's action (other-type neurons, OT, Figure 22c,d) although the monkey neither moved nor prepared to move in these trials (Figure 18a, b), and the majority (n= 40, 48%) discharged during the presentation of the object both when it was targeted by the monkey's and by the experimenter's action (self-and-other type neurons, SOT, Figure 22e, f). In this latter set of neurons, we could quantitatively assess the relationship between neural processing of object as a target for self-action (execution task) or another agent's action (observation task).

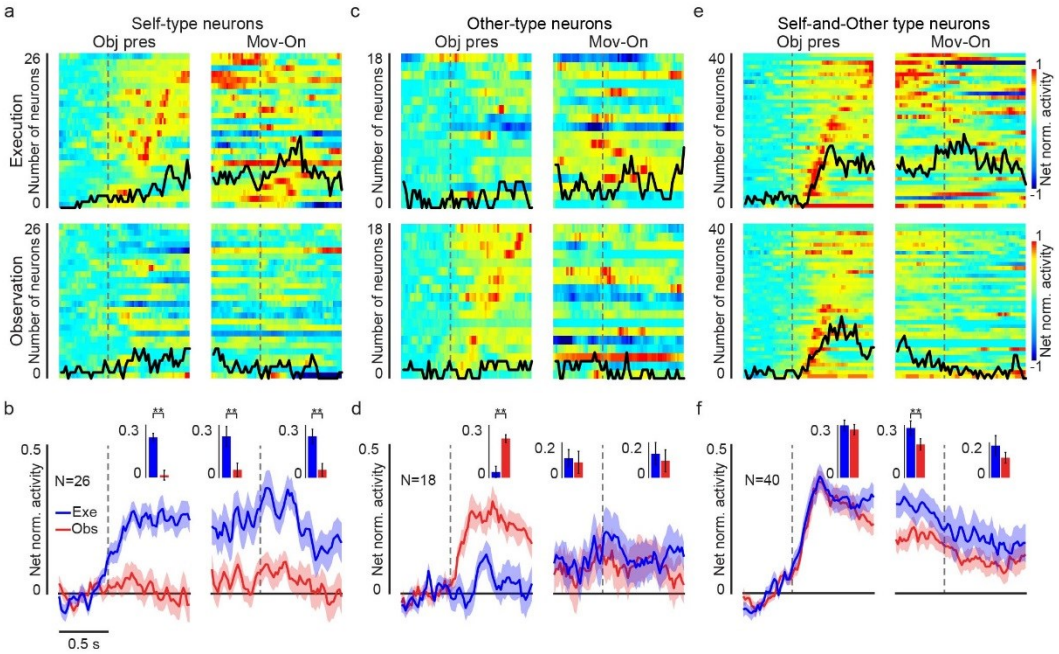

Figure 22. Single neuron and population activity of self, other, and self-and-other type object-related neurons. (a, c and e) Heat map plots of the temporal activation profile of single unit net normalized activity for ST (a), OT (c), and SOT (e) object-related neurons. Neurons are ordered based on the timing of their peak of activity in the object presentation period of the execution task, in case of ST and SOT neurons (panels a and e), or of the observation task, in case of OT neurons (panel c), with the earliest on the bottom for all plots. (b, d and f) Time course and intensity of the mean net normalized population activity for the three sets of neurons shown in the correspondent panels above, during the execution

(blue) and observation (red) task. Paired-samples t-tests * $p < 0.05$, ** $p<0.01$. All other conventions as in Figure 20.

The object presentation response of two different SOT object-related neurons recorded during Go trials of the execution and observation tasks is shown in Figure 23a. The discharge profile and object selectivity of Neuron 1 are impressively similar when different agents (monkey or experimenter) had to grasp it. This pattern of activity may thus reflect an agent-independent coding of a pure object affordance (Pezzulo & Cisek, 2016). Neuron 2 exhibits a different behavior, being active in both tasks but showing a stronger modulation when the object was a target for the experimenter than for the monkey. This pattern of activity may thus correspond to an agent-based representation of the object. To quantitatively assess the overall relevance of these two different modes of object processing by SOT object-related neurons, we statistically analyzed parameters of their activity in the two contexts (execution and observation). We found that peaks of activity (Figure 23b), their timing (Figure 23c), bursts' duration (Figure 23d) and preferences for objects (Figure 23e) were all highly correlated and not significantly different between task execution and observation, suggesting a remarkable degree of similarity between the overall activity pattern during the two conditions. Cross-modal decoding carried out on this set of neurons provided further support to the hypothesis that they may encode the object's affordance both when it was targeted by self and by another's action (Figure 23f). Indeed, by training the classifier with input data collected during the execution and observation tasks, it could discriminate among objects equally well and largely above-chance level with both execution (Figure 23f, Exe) and observation (Figure 23f, Obs) data, suggesting that visual information on objects can be extracted with similar degree of accuracy regardless of the agent (self or other) to which it is addressed. To directly test possible agent-invariant coding of visually presented objects we applied a decoding algorithm to test whether it could discriminate the agent (self or other) to which the target was addressed based on SOT object-related neuron activity (see Methods). We found highly over-chance agent decoding accuracy (Figure 23g), indicating that, despite the remarkable similarities between their representations of objects targeted by self or other agents, even SOT object-related neuron activity reflects agent selectivity.

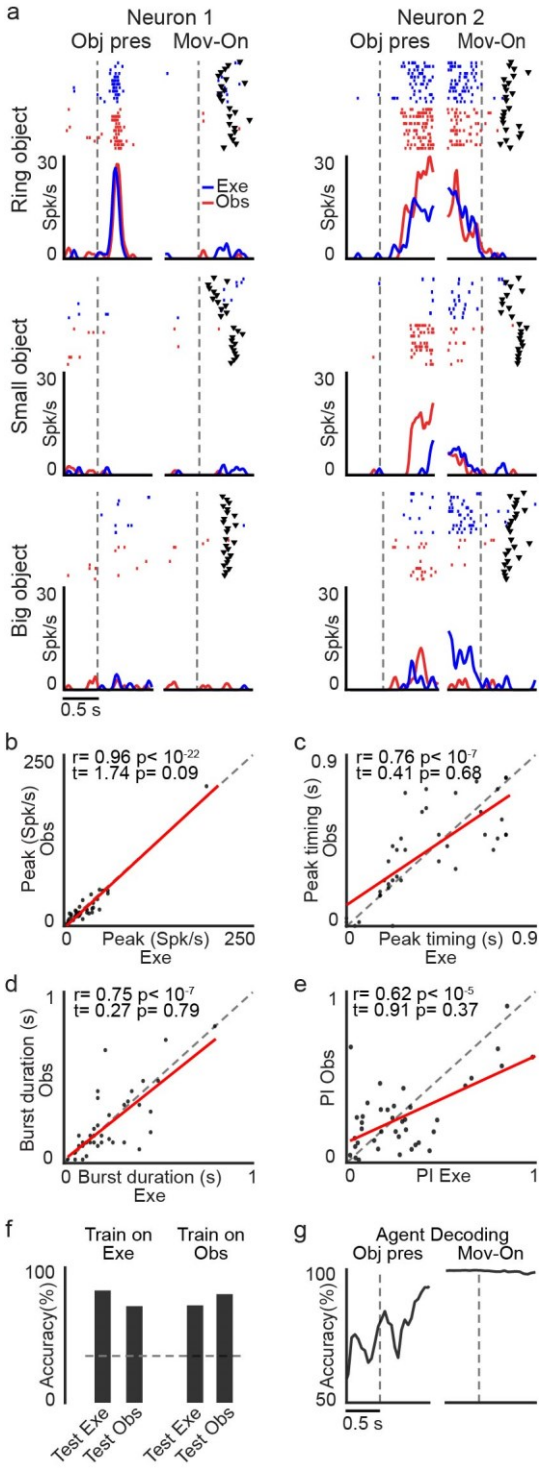

Figure 23. Relationship between SOT object-related neurons response to the visual presentation of the target for self (execution task) or other's (observation task) action. (a) Single neuron responses (raster and line plot) during task execution (Exe, blue) and observation (Obs, red) aligned (vertical dashed lines) on object presentation (Obj pres) and (after the gap) movement onset (Mov-on) with the three different objects as target. (b) Correlation plot of peak activity (in spikes/second) of the same cells (n=69) in the 0.8 s following Obj pres in the execution and observation task. (c) Correlation plot of peak activity timing of the same cells during the execution and observation task (same period as b). (d) Correlation plot of burst duration (see Methods) of the same cells during object presentation in the execution and observation task. (e) Correlation plot of object preference index (PI, see Methods) calculated for the same cells on the responses during object

presentation in the execution and observation task. (f) Accuracy in the classification of the target object (ring, small and big cones) during object presentation in execution and observation trials based on a training of the classifier carried out with SOT object-related neuron activity collected during either one of the two tasks. (g) Time course of the agent decoding accuracy based on SOT object-related neuron activity collected during task execution and observation. All conventions are as in Figure 21.

Object-related neuron activity is strictly constrained to the monkey's peripersonal space

In principle, "being at hand" could be not only necessary, but even sufficient to induce an automatic retrieval of an object's motor affordance in an observer's brain, regardless of whether the hand belongs to the observer or someone else (Cardellicchio *et al.*, 2013). To test whether this hypothesis applies to area F6 object-related neurons, we compared neuronal responses to a visually presented object when it was a target 1) for the monkey's own action, 2) for the experimenter's action performed in the monkey's peripersonal space (see Figure 3b), and 3) for the experimenter's action performed in the monkey's extrapersonal space (see Figure 3c). It is clear that, regardless of the neuronal subpopulation (Figure 24a-c), object related neurons do not discharge when the visually presented object is located in the monkey's extrapersonal space. This is also evident for SOT object-related neurons (Figure 24c), indicating that objects are represented as a potential target for monkey's own action.

Furthermore, object presentation responses are stronger during Go relative to No-Go condition in all the three neuronal subpopulations. It is worth to note that in both subpopulations that encode the object when it is targeted by another agent (OT and SOT), the response reflects the same enhancement for the Go condition even during the observation task, when the experimenter, not the monkey, will grasp the object. This is particularly interesting for SOT object-related neurons, where we have already shown evidence of a close correspondence between the neuronal coding of object when it is a target for self and other's action (Figure 23).

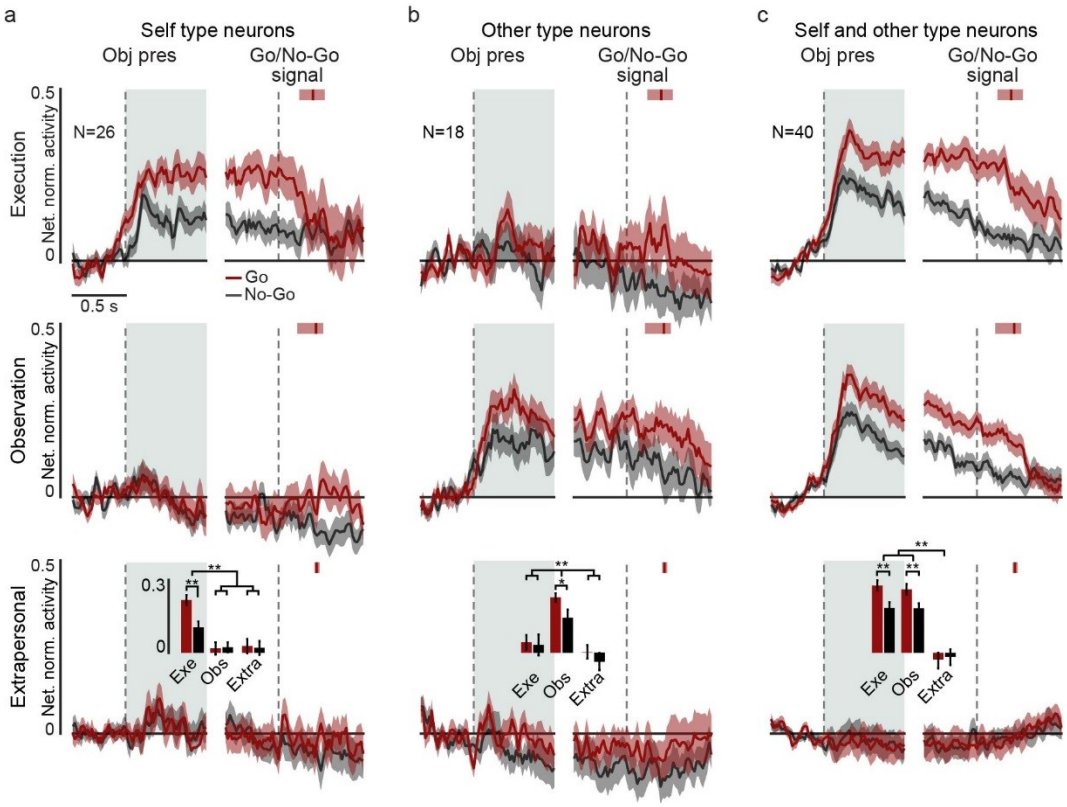

Figure 24. Space-constrained activity of object-related neurons. Population activity of ST (A), OT (B) and OST (C) neurons during task execution (top row), task observation in the monkey's peripersonal (middle row) and extrapersonal (bottom row) space during Go (red) and No-Go (gray) conditions. The activity is aligned (first dashed line on the left of each panel) to object presentation (Obj pres), and then to the Go/No-Go signal (second dashed line on the right of each panel). The response profile has been computed by averaging the response to the three different objects. The shading around each line indicates 1 standard error. Histograms in the bottom row represent the mean activity in each object presentation epoch (light-blue region following object presentation), compared among tasks with a 2x3 repeated measures ANOVA (factors: Condition and Task) followed by Bonferroni post-hoc test, * $p < 0.05$, ** $p<0.01$. Red vertical markers after Go/No-Go signal represent the median movement onset time, with indication of the 25th and 75th percentile (shaded area around each marker).

Agent-based population codes dynamically emerge from object presentation to action execution

To assess the integrated contribution of F6 neurons to agent-based representations of objects and actions during task unfolding, we next applied cross-modal neural decoding methods to population data (Meyers, 2013). All 306 neurons recorded from the two monkeys (111 neurons from M1 and 195 from M2) were included, using as unique selection criterion the one of being well-isolated cells based on standard parameters (see Methods). A pattern classifier was first trained on a set of data collected in one task condition (execution, observation, and extrapersonal) to discriminate between Go and No-Go trials (Figure 25a) and the type of object (Figure 25b).

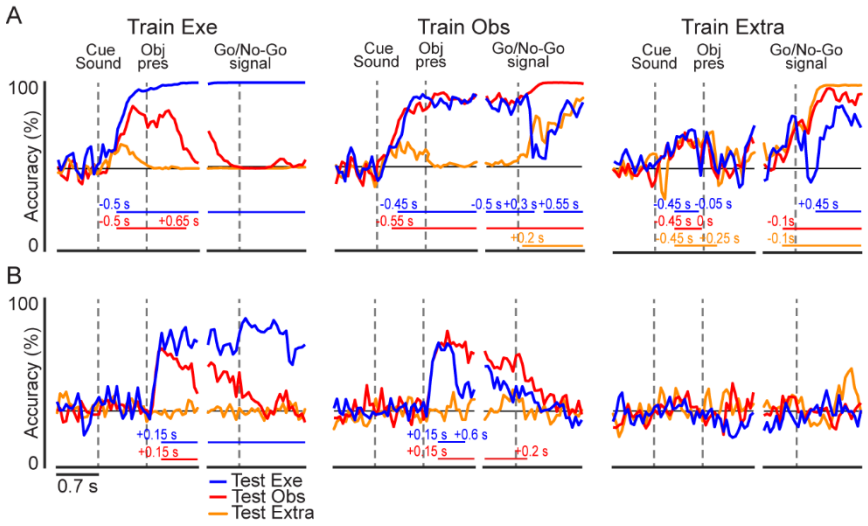

Figure 25. Cross-modal decoding of target object and Go/No-Go condition from area F6 population activity. (A) Classification accuracy over time of Go and No-Go trials in three different contexts, as a result of a classifier trained with a subset of data recorded in the execution (Exe), observation (Obs), or extrapersonal (Extra) task. The horizontal lines in the lower part of the plot indicate the time period during which the decoding accuracy was significantly and steadily above chance for at least 250 ms (see Methods). (B) Classification accuracy over time of the type of object/grip type. Conventions as in (A). Fig. 26 and 27 illustrate the results of analysis of individual animals.

Then the classifier's decoding performance was tested on each condition to investigate whether, and to what extent, the population code generalizes across agents. The analyses were performed on data from each monkey, separately (Figure 26 and 27), but since the results were similar, here the data from the two animals have been combined. Figure 26 shows decoding from M1.

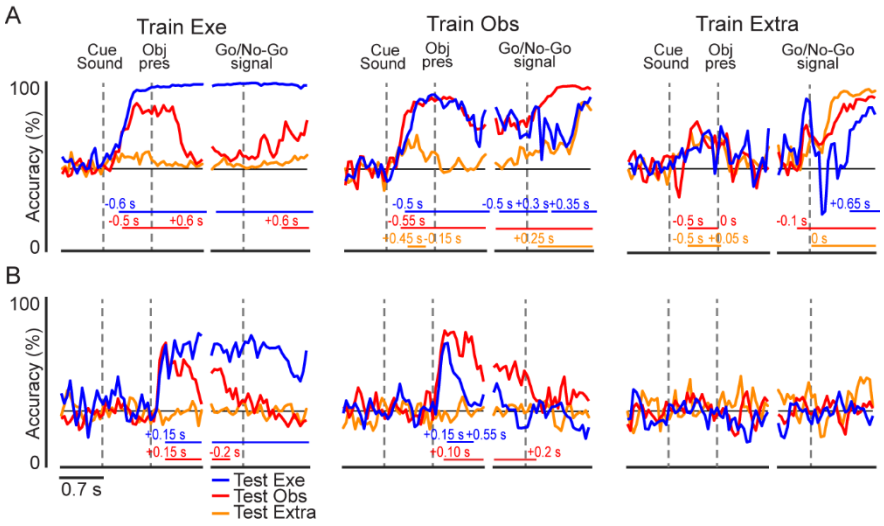

Figure 26. Cross-modal decoding of target object and Go/No-Go condition from area F6 population activity of M1. (A-C) Classification accuracy over time of Go and No-Go trials in three different contexts, as a result of the classifier trained with a subset of data recorded in the execution (Exe), observation (Obs), or extrapersonal (Extra) task. The dashed lines in the lower part of the plot show the time period during which the decoding accuracy was significantly and steadily above chance for at least 300 ms (see Methods). (D-F) Classification accuracy over time of the type of object. Conventions as in (A-C).

Figure 27 shows decoding from M2.

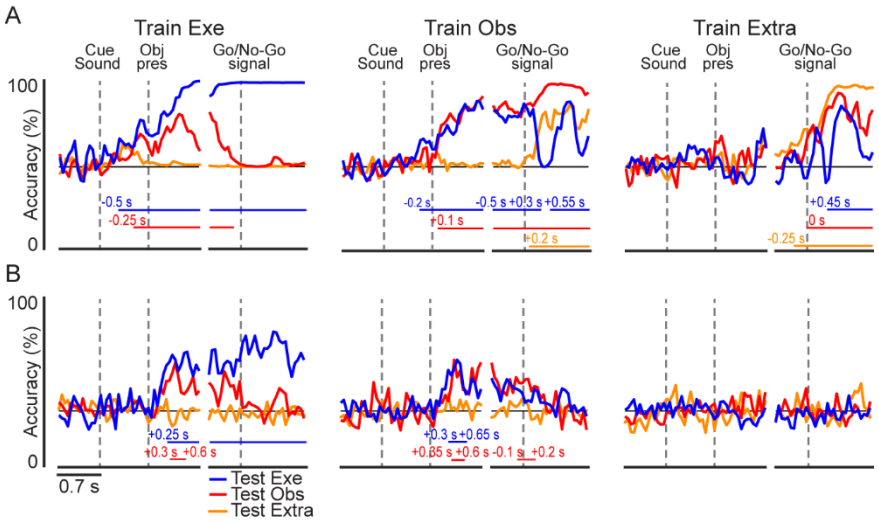

Figure 27. Cross-modal decoding of target object and Go/No-Go condition from area F6 population activity of M2. (A-C) Classification accuracy over time of Go and No-Go trials in three different contexts, as a result of a classifier trained with a subset of data recorded in the execution (Exe), observation (Obs), or extrapersonal (Extra) task. The dashed lines in the lower part of the plot show the time period during which the decoding accuracy was significantly and steadily above chance for at least 300 ms (see Methods). (D-F) Classification accuracy over time of the type of object. Conventions as in (A-C).

After training the classifier on execution data, both Go/No-Go (Train Exe, Figure 25a) and object (Train Exe, Figure 25b) decoding accuracy were significant throughout the object presentation (pre-movement) period when tested with execution and observation, but not extrapersonal, data. A similar pattern was confirmed by training the classifier on observation data (Train Obs, Figure 25a, b) but not on extrapersonal data (Train Extra, Figure 25a, b), indicating that information conveyed by the cue sound and the target object can generalize between different agents, provided that they share the same operative space.

From the Go/No-Go signal onward, the classifier had to discriminate between performed and withheld actions (Figure 25a) and grip types (Figure 25b). Concerning action decoding (Figure 25a, after the gaps), the classifier trained on execution data (Train Exe) could not decode other's observed action in any other task contexts (Test Obs and Test Extra). In contrast, when trained on either observation (Train Obs) or extrapersonal data (Train Extra), it could reach significant decoding accuracy, although with clear-cut differences, with both execution (Exe) and observation (Obs and Extra) data. This unidirectional visual-to-motor generalization of neural representation of actions suggests that somato-motor bodily signals determine agent specificity. Noteworthy, cross-modal decoding of grip type (Figure 25b, after the gaps) did not show any evidence of generalization between the neural code associated with self- and other-action, suggesting that grip representation in area F6 completely depends on somato-motor rather than visual signal, and it cannot be achieved thorough the observation of other's action. It is worth to note that even when all object-related neurons are excluded from the population, it is still possible to decode the visually presented object/grip type across tasks with similar, though slightly reduced, accuracy (Figure 28). This finding suggests that, despite the crucial contribution of specific neuronal classes, the generalization of object representations across self and other is a computationally distributed function that does not critically depend on a selected population of neurons.

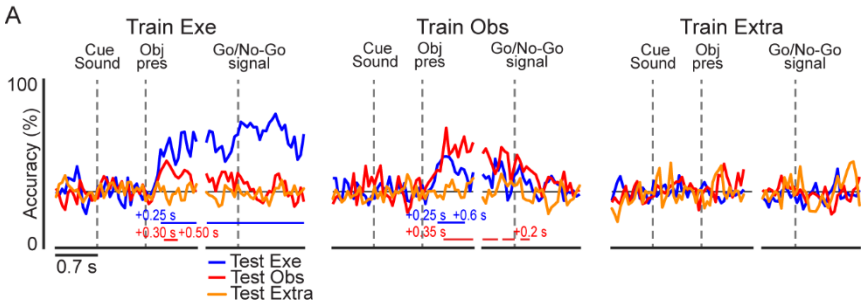

Figure 28. Cross-modal decoding of target object from area F6 population activity after exclusion of all object-related neurons (n=222). Conventions as in Figure 25.

In summary, whereas area F6 appears to integrate auditory and visual information prior to movement onset to generate an agent-shared signal specifying "whether" and "how" self or other's action will occur in the monkey' peripersonal space, it then switches to a broader agent-based goal attainment signal during action unfolding.

4. DISCUSSION

According to several neurophysiological studies, the pre-supplementary motor cortex plays a crucial role in complex sequential and cognitive processes underlying simple *movements* required as a response in a behavioral task (Tanji, 2001; Akkal *et al.*, 2004; Shima & Tanji, 2006; Nakajima *et al.*, 2009; Lucchetti *et al.*, 2012). Another view maintains that the presupplementary motor cortex is involved in the specification of "whether" and "when" to perform an intended action (Haggard, 2008), particularly in complex "cognitive" situations (Nachev *et al.*, 2008). By contrast, encoding 'what' an action should be and 'how' it must be performed is thought to involve the dorso-lateral parieto-frontal system (Rizzolatti *et al.*, 2014).

Here, we show for the first time that 1) area F6 neurons can contribute to the visuomotor processing of objects and to the encoding of how grasping *actions* must be performed during a go/no-go visuomotor task (Exp 1); 2) area F6 hosts distinct neuronal population of visual/visuomotor and purely motor neurons that form two rather dichotomic sets of neurons, with firing pattern specificities that greatly differentiate the visuomotor processes of F6 from those of F5, studied in the same animals and with the same tasks; 3) object processing in F6, as previously shown for action representations, is markedly agent-specific, allowing to predict since the object presentation phase who may grasp the object, whether it will be grasped depending on contextual cues, and using what type of grip.

Altogether, these findings extend to F6 the cortical grasping network, to date mostly limited to ventral premotor and parietal areas (Janssen & Scherberger, 2015; Borra *et al.*, 2017; Fattori *et al.*, 2017), and further demonstrate the role of this area in social functions (Yoshida *et al.*, 2012; Sliwa & Freiwald, 2017).

The dominant, text-book view maintains the presupplementary motor area F6 is involved in generating initiation signal for actions to be performed, contributing to specify temporal and sequential aspects of forthcoming behavior with low selectivity for details of the motor acts, such a as the grip type and the most distal components of manual actions (Rizzolatti & Luppino, 2001; Nachev *et al.*, 2008; Kandel, 2012). These details are generally thought to be encoded in the

dorso-ventral premotor and parietal regions. Our findings challenge this view by indicating that a subset of F6 neurons can exhibit object-selective visual and motor responses with remarkable specificity for the object/grip type. Most interestingly, visuomotor and purely motor F6 neurons appear to form two functionally distinct populations, in striking contrast to the dynamic visual-to-motor processing displayed by F5 visuomotor single-neuron and population activity. Furthermore, the visual processing of objects by area F6 neurons appears to be context-dependent, because neuronal selectivity was stronger when target presentation occurred in the context of go trials relative to no-go trials, and was completely abolished when, in spite of the instruction to go, a transparent barrier was interposed between the monkey's hand and the target, preventing the animal from reaching it. Altogether, these findings suggest that F6 visual activity can provide a motor representation of the impending object-directed action, which is conditional upon both the monkey's intention and possibility to perform it.

Using an additional condition even more surprisingly neuronal properties were revealed. Comparing the visuo-motor properties of F6 neurons while the animal was performing the task with those to when the animal was observing another agent doing the same we found neurons coding for both conditions. The results provide new evidence for an accurate and agent-shared representation of observed graspable objects, which dynamically switches to a broader agent-based goal attainment signal during action unfolding.

One of the most striking findings in the anatomical literature concerning area F6 is that, as compared with the adjacent supplementary motor area F3, it completely lacks direct connections with the spinal cord and the primary motor cortex (He *et al.*, 1993; Luppino *et al.*, 1993), in line with its low electrical excitability demonstrated by both the present and previous (Luppino *et al.*, 1991b) studies. Hence, its contribution to grasping actions has to be mediated by other anatomically connected areas.

Anatomical connections with area F6 have in fact been demonstrated for all the main premotor (Matelli *et al.*, 1986; Luppino *et al.*, 1993; Gerbella *et al.*, 2011) as well as parietal (Luppino *et al.*, 1993; Lewis & Van Essen, 2000; Rozzi *et al.*, 2006; Gamberini *et al.*, 2009) nodes of the grasping network. Furthermore, F6 is

consistently linked with the prefrontal cortex, particularly with the intermediate part of the convexity and bank portions of both dorsal (Saleem *et al.*, 2014) and ventral (Gerbella *et al.*, 2013) area 46. Interestingly, in this latter sector neurons related to reaching-grasping actions have been recently described (Simone *et al.*, 2015), and have been shown to exhibit visuomotor properties and context-dependent modulations (Bruni *et al.*, 2015). Finally, area F6 is also heavily connected with sectors of the basal ganglia (Parthasarathy *et al.*, 1992; Takada *et al.*, 2001; Bruni *et al.*, 2018) where neurons with hand-related motor responses have been described (Crutcher & DeLong, 1984b; a; Alexander & DeLong, 1985b; a). In sum, anatomical data strongly support the possibility that F6 plays a crucial role in reaching-grasping actions by integrating a wide range of information and influencing, both directly and indirectly, the processing operations carried out by the core areas of the grasping network.

The findings of the present study provide direct functional evidence in favor of this view by demonstrating that almost 26% of F6 task-related neurons display object/grip selectivity. Although this percentage is clearly lower than that obtained for area F5 (41%), there are several additional similarities between object processing in the two areas, strengthening the idea of their functional interplay. First, we showed that neuronal discharge and object selectivity of F6 purely motor neurons were the same during grasping in both the light and the dark, indicating that their activity truly reflects a motor encoding of the hand grip, as previously shown for F5 (Raos *et al.*, 2006; Gamberini *et al.*, 2009; Schaffelhofer *et al.*, 2015). Second, both the response to visual presentation and object selectivity of F6 visuomotor neurons were stronger during go trials, which is consistent with previous findings in F5 (Raos *et al.*, 2006; Bonini *et al.*, 2014b), and suggests that visuomotor neurons of both areas encode visually presented objects in a motor format. Third, the barrier test revealed that object selectivity was abolished when a transparent barrier was interposed between the monkey's hand and the target, as demonstrated for area F5 visuomotor neurons (Bonini *et al.*, 2014b), confirming both areas underlie a 'pragmatic description' of observed objects.

In spite of the functional analogies so far described and the tight reciprocal anatomical connections between F6 and F5 that could account for them, it is unlikely that these two areas provide a similar contribution to grasping actions. For

example, it has been directly demonstrated that the inactivation of area F5 in monkeys impairs visually guided grasping of objects, providing causal evidence that this region plays a crucial role in controlling the hand shape for appropriately interacting with the target (Fogassi *et al.*, 2001). In contrast, reaching-grasping actions are virtually unimpaired following large lesions of the pre-supplementary motor cortex (Brinkman & Porter, 1983; Thaler *et al.*, 1995). These findings would suggest normal manual behavior is the outcome of fine control from area F5 and F6 has smaller relationship with the fine motor tuning. Instead, the mesial area may controls the movements through controlling area F5 instead. Our data reveal the existence, in area F6, of an articulated visuomotor representation of objects and how they can be grasped. The direct comparison with the neuronal properties of area F5 allowed us to elucidate the specific contribution of F6 to reaching-grasping actions.

Convergent evidence from several studies indicates the existence of a typical visual-to-motor response pattern in all the parietal (Sakata *et al.*, 1995; Baumann *et al.*, 2009; Fattori *et al.*, 2012; Fattori *et al.*, 2017) and premotor (Murata *et al.*, 1997; Raos *et al.*, 2004; Raos *et al.*, 2006; Fluet *et al.*, 2010; Bonini *et al.*, 2014b; Vargas-Irwin *et al.*, 2015) nodes of the dorsolateral grasping network, particularly in F5 (Figure 15). The visual-to-motor response, originally investigated on the AIP-F5 network, has been classically deemed to reflect the visuomotor transformation of objects' physical properties into the motor acts most appropriate for interacting with them (Jeannerod *et al.*, 1995). However, based on the fundamental differences we found between the single neuron and population activity of F6 and F5, it appears unlikely that F6 neurons play a role in visuomotor transformation. Instead, an interesting and more plausible interpretation can be suggested by considering the specific aspects of the neuronal visuomotor processing that characterize the two areas.

Our findings show that area F6 single neurons peak relatively earlier and display shorter bursts of phasic activity relative to those of F5 (Figure 16), which, in contrast, exhibit a more sustained activity tuned on the hand-object interaction. At the population level, these differences translate into even more clear-cut evidence: though being anatomically intermingled, like those of F5 (Bonini *et al.*, 2014b), visuomotor and purely motor F6 neurons form two functionally distinct populations. The former provides mainly a visual processing of the object (Figure

16b and 17a), whereas the latter underlies a motor encoding of the grip type (Figure 16b and 17c). In line with this difference, we also found a set of F6 neurons with purely visual response properties (Table 1), which are virtually absent in area F5. Interestingly, area F6 purely visual neurons can also display contextual selectivity for go or no-go trials (see the example Neuron 1 in Figure 12a), confirming the general role of F6 visually triggered neurons in motor-related functions. More importantly, we observed a striking difference in the tuning for specific objects between the two areas. Indeed, F6 exhibited a bias in its visual and preparatory activity for the ring (i.e., hook grip), whereas F5 displayed a strong motor bias in favor of the small cone (i.e., precision grip). This finding suggests that whereas in F6 the processing of over-learned visuomotor associations prevails, in F5 there is a preferential coding of the visuomotor transformations related to the grip types belonging to the monkey's natural behavioral repertoire (Macfarlane & Graziano, 2009).

How could visuomotor transformation and association processes interact? Typically, the same object can offer multiple grip affordances. Among them, we select the most appropriate depending on the current contextual situation, the goal we are pursuing, or specific instructions. Interestingly, Fluet and coworkers (Fluet *et al.*, 2010) showed that ventral premotor neuronal representations of specific grip types (i.e., precision or power grip) to be employed for grasping the same handle can be triggered by the presentation of abstract visual cues (white or green spots of light) previously associated with the instructed grip type. Furthermore, using a similar paradigm, Vargas-Irwin and coworkers (Vargas-Irwin *et al.*, 2015) revealed that premotor neurons can dynamically integrate information related to the visual features of an observed object with the subsequently presented instructional cues for how to grasp it. Therefore, it is clear that in area F5 the visuomotor transformation of an object's visual features into the motor plans required for grasping it are flexibly modulated by learned visuomotor associations. The present findings strongly suggest that F6 encodes visuomotor associations between specific elements of contextual information, likely conveyed by the prefrontal cortex, and motor representations of reaching-grasping actions. By playing a role in driving premotor activity, F6 could contribute to add contextual flexibility to the visuo-motor transformations of the cortical grasping network.

As reported by previous single-neuron studies investigating reaching actions (Yoshida *et al.*, 2011; Falcone *et al.*, 2017), by comparing the activity between execution and observation tasks we found three main categories of action-related neurons: motor neurons becoming active during object grasping (ST neurons), visually-responsive neurons discharging selectively during other's observed action (OT neurons), and visuomotor neurons discharging during both self- and other's action (SOT neurons). This latter set of neurons behave as the classical "mirror neurons" reported in several nodes of the cortical grasping network (Bonini, 2016). However, the two previous studies carried out on F6, mostly focused on "other-type" neurons, considered as a necessary complement of mirror neurons to make self-other distinction possible. In contrast, here we demonstrated considerable differences between the visual and motor discharge even among neurons with mirror properties (SOT), not only in terms of discharge pattern but also in terms of grip selectivity. Indeed, whereas grip type information was clearly represented by their motor discharge in line with recent findings (Lanzilotto *et al.*, 2016), by applying cross-modal decoding methods we found no evidence of a shared visuo-motor code for the type of grip in SOT neuron. Furthermore, the same neural decoding approach could robustly discriminate SOT neuron activity associated with self and others' action, demonstrating that "sharedness does not mean identicality" (Decety & Sommerville, 2003) in the neural codes for action representation, at least in area F6.

Whereas F6 action-related neurons cannot specify "how" another's action will be performed, here we found that this information is encoded by object-related neurons. Indeed, as previously reported for action-related neurons, we found distinct sets of neurons encoding visually presented objects when they were targeted by the monkey's own action (ST neurons), by the experimenter's action (OT neurons), or both (SOT neurons). Self-type neurons likely represent the object as a potential target for the monkey, as previously hypothesized for visuomotor neurons in several other brain areas (Murata *et al.*, 1997; Raos *et al.*, 2004; Raos *et al.*, 2006; Schaffelhofer & Scherberger, 2016), including F6 (Lanzilotto *et al.*, 2016). In line with this interpretation, they are characterized by stronger activity during Go- relative to No-Go trials, robust and sustained visual-to-motor activity, and clear-cut object/grip selectivity. In contrast, OT neurons do not appear to represent the object

features, but rather a broader predictive signal about another's impending action, as previously hypothesized for some visuomotor neurons recorded from area F5 (Bonini *et al.*, 2014b). Indeed, they show stronger activation during Go relative to No-Go trials, a relatively weak visual-to-motor activity and, most importantly, no significant object/grip selectivity.

Self-and-other type object-related neurons are certainly the most intriguing ones. Most of these cells and their overall population activity showed an impressive similarity in terms of temporal activation pattern and object selectivity during the execution and observation task. By applying cross-modal decoding methods to this neuronal population, in striking contrast with the results obtained with action-related neurons, we found robust evidence of a shared neural code underlying the representation of objects targeted by self- and other-action. At first glance, these findings may lead one to consider these neurons as the classical visuomotor object-related neurons, which respond to a visually presented graspable object in the same way every time the monkey is facing it (Sakata *et al.*, 1995; Murata *et al.*, 1997): in other terms, they may be simply representing the object's affordances *for the monkey*, with no agent-specificity. Against this idea, we showed that a classifier could robustly discriminate self- from other-trials based on SOT object-related neuron activity. Furthermore, the same enhanced object presentation response characterizing Go relative to No-Go trials in the execution task was also observed in the observation task, where the monkey remained completely still in both Go and No-Go conditions. Therefore, we suggest that a mechanism similar to action mirroring exists in area F6 for graspable objects as well, that can be named as "object mirroring". As compared to action mirroring, "object mirroring" appears to convey a richer and more precise information as to whether a reaching-grasping action will be taken, how it will be done, and who is about to perform it, enabling a subject to exploit part of the same neural circuit both to plan object-directed actions and to predict the actions of others long before any observable movement onset.

Predicting other's action is usually possible even when the agent is located far from us, or on the virtual space of a screen (Cisek & Kalaska, 2004; Cardellicchio *et al.*, 2013; Hasson & Frith, 2016), whereas the discharge of object-related neurons in area F6 appears to be strictly constrained to the observer's

peripersonal space. Future studies should investigate whether a similar neuronal mechanism with space-invariant features exists in other brain areas. Nonetheless, it seems reasonable to propose that the object mirroring mechanism described here in area F6 does not play a general role in action prediction as previously described in the ventral premotor cortex (Bonini *et al.*, 2014b; Maranesi *et al.*, 2014b; Mazurek *et al.*, 2018), but it may rather allow the representation of specific object-directed behaviors in a shared space for self and others' impending action.

To better understand the link between object- and action-mirroring mechanisms in area F6, we employed cross-modal neural decoding methods to dynamically explore the possible generalization of the population code from self to other (and vice versa). Our results show that following an early, mostly agent-shared representation of information specifying "whether" and "how" an object will be grasped, the population code progressively switches to a mostly agent-based goal attainment signal, devoid of any object/grip selectivity during other's action observation. It is worth noting that the population code does reflect information on the grip type, but only during action execution, indicating a strict dependency of this information from a somatosensory feedback or motor-related signal from other anatomically connected areas (Luppino *et al.*, 1993). These signals contribute to radically differentiate the activity related to self and other's action.

Summing up, we provide evidence of a novel neural mechanism that allows recruiting the same motor representation of an object either for planning actions or to precisely predict how another agent will act when facing that object in the same context. Our findings support the idea that object-mirroring mechanism plays a more important role than action mirroring in simple and direct forms of context-based action prediction.

Conclusions

The present study is the first evidence highlighting similar functional properties between area F6 and regions of the so called "lateral grasping network" (Borra *et al.*, 2017). Based on anatomical data area F6 has been defined as "pre-fronto dependent region" (Rizzolatti & Luppino, 2001). For years it has been typically associated with temporal and sequential aspects of motor commands (Rizzolatti *et*

al., 1990b; Nachev *et al.*, 2008). However this study is the first one to investigate F6 single neurons during manipulative actions. The result clearly shows area F6 hosts also visuomotor neurons, coding "the way" an action is performed. More interestingly this study demonstrates that visuomotor representation can be shared between agents. Some of the visuomotor neurons encode task information (i.e. visual features of the object and contextual information) in a similar way when the subject performed the task or observed another agent performing the same. One possible function of such a mirror mechanism is the ability of predicting others action's. Having a shared action representation, triggered by object features and contextual information, may represent a fast way to generalize planning mechanisms to predict other's behavior. This mechanism, though, appears to be spatially constrained to the peripersonal space, at least in area F6. It might be possible similar "contextual-based" mirror mechanisms can be find in other regions, connected with F6, with higher level of complexity (i.e. more abstract, extrapersonal space, etc.). Such abstract mirroring mechanisms may be the neural correlates for other behaviors prediction's with no need for high order inferential reasoning.

5. REFERENCES

Akkal, D., Escola, L., Bioulac, B. & Burbaud, P. (2004) Time predictability modulates pre-supplementary motor area neuronal activity. *Neuroreport*, **15**, 1283-1286.

Alexander, G.E. & DeLong, M.R. (1985a) Microstimulation of the primate neostriatum. I. Physiological properties of striatal microexcitable zones. *Journal of neurophysiology*, **53**, 1401-1416.

Alexander, G.E. & DeLong, M.R. (1985b) Microstimulation of the primate neostriatum. II. Somatotopic organization of striatal microexcitable zones and their relation to neuronal response properties. *Journal of neurophysiology*, **53**, 1417-1430.

Barz, F., Paul, O. & Ruther, P. (2014) Modular assembly concept for 3D neural probe prototypes offering high freedom of design and alignment precision. *Conference proceedings : ... Annual International Conference of the IEEE Engineering in Medicine and Biology Society. IEEE Engineering in Medicine and Biology Society. Annual Conference*, **2014**, 3977-3980.

Baumann, M.A., Fluet, M.C. & Scherberger, H. (2009) Context-specific grasp movement representation in the macaque anterior intraparietal area. *The Journal of neuroscience : the official journal of the Society for Neuroscience*, **29**, 6436-6448.

Belmalih, A., Borra, E., Contini, M., Gerbella, M., Rozzi, S. & Luppino, G. (2007) A multiarchitectonic approach for the definition of functionally distinct areas and domains in the monkey frontal lobe. *Journal of anatomy*, **211**, 199-211.

Bonini, L. (2016) The Extended Mirror Neuron Network: Anatomy, Origin, and Functions. *The Neuroscientist : a review journal bringing neurobiology, neurology and psychiatry*.

Bonini, L. & Ferrari, P.F. (2011) Evolution of mirror systems: a simple mechanism for complex cognitive functions. *Annals of the New York Academy of Sciences*, **1225**, 166-175.

Bonini, L., Maranesi, M., Livi, A., Bruni, S., Fogassi, L., Holzhammer, T., Paul, O. & Ruther, P. (2014a) Application of floating silicon-based linear multielectrode

arrays for acute recording of single neuron activity in awake behaving monkeys. *Biomedizinische Technik. Biomedical engineering*, **59**, 273-281.

Bonini, L., Maranesi, M., Livi, A., Fogassi, L. & Rizzolatti, G. (2014b) Space-dependent representation of objects and other's action in monkey ventral premotor grasping neurons. *The Journal of neuroscience : the official journal of the Society for Neuroscience*, **34**, 4108-4119.

Bonini, L., Maranesi, M., Livi, A., Fogassi, L. & Rizzolatti, G. (2014c) Ventral premotor neurons encoding representations of action during self and others' inaction. *Current biology : CB*, **24**, 1611-1614.

Bonini, L., Rozzi, S., Serventi, F.U., Simone, L., Ferrari, P.F. & Fogassi, L. (2010) Ventral premotor and inferior parietal cortices make distinct contribution to action organization and intention understanding. *Cereb Cortex*, **20**, 1372-1385.

Bonini, L., Ugolotti Serventi, F., Bruni, S., Maranesi, M., Bimbi, M., Simone, L., Rozzi, S., Ferrari, P.F. & Fogassi, L. (2012) Selectivity for grip type and action goal in macaque inferior parietal and ventral premotor grasping neurons. *Journal of neurophysiology*, **108**, 1607-1619.

Borra, E., Belmalih, A., Calzavara, R., Gerbella, M., Murata, A., Rozzi, S. & Luppino, G. (2008) Cortical connections of the macaque anterior intraparietal (AIP) area. *Cereb Cortex*, **18**, 1094-1111.

Borra, E., Belmalih, A., Gerbella, M., Rozzi, S. & Luppino, G. (2010) Projections of the hand field of the macaque ventral premotor area F5 to the brainstem and spinal cord. *The Journal of comparative neurology*, **518**, 2570-2591.

Borra, E., Gerbella, M., Rozzi, S. & Luppino, G. (2017) The macaque lateral grasping network: A neural substrate for generating purposeful hand actions. *Neuroscience and biobehavioral reviews*, **75**, 65-90.

Brinkman, C. & Porter, R. (1983) Supplementary motor area and premotor area of monkey cerebral cortex: functional organization and activities of single neurons during performance of a learned movement. *Advances in neurology*, **39**, 393-420.

Bruni, S., Gerbella, M., Bonini, L., Borra, E., Coude, G., Ferrari, P.F., Fogassi, L., Maranesi, M., Roda, F., Simone, L., Serventi, F.U. & Rozzi, S. (2018) Cortical and subcortical connections of parietal and premotor nodes of the monkey hand mirror neuron network. *Brain structure & function*, **223**, 1713-1729.

Bruni, S., Giorgetti, V., Bonini, L. & Fogassi, L. (2015) Processing and Integration of Contextual Information in Monkey Ventrolateral Prefrontal Neurons during Selection and Execution of Goal-Directed Manipulative Actions. *The Journal of neuroscience : the official journal of the Society for Neuroscience*, **35**, 11877-11890.

Caggiano, V., Fogassi, L., Rizzolatti, G., Casile, A., Giese, M.A. & Thier, P. (2012) Mirror neurons encode the subjective value of an observed action. *Proceedings of the National Academy of Sciences of the United States of America*, **109**, 11848-11853.

Caggiano, V., Fogassi, L., Rizzolatti, G., Thier, P. & Casile, A. (2009) Mirror neurons differentially encode the peripersonal and extrapersonal space of monkeys. *Science*, **324**, 403-406.

Cardellicchio, P., Sinigaglia, C. & Costantini, M. (2013) Grasping affordances with the other's hand: a TMS study. *Social cognitive and affective neuroscience*, **8**, 455-459.

Cisek, P. (2007) Cortical mechanisms of action selection: the affordance competition hypothesis. *Philosophical transactions of the Royal Society of London. Series B, Biological sciences*, **362**, 1585-1599.

Cisek, P. & Kalaska, J.F. (2004) Neural correlates of mental rehearsal in dorsal premotor cortex. *Nature*, **431**, 993-996.

Cisek, P. & Kalaska, J.F. (2010) Neural mechanisms for interacting with a world full of action choices. *Annual review of neuroscience*, **33**, 269-298.

Cooke, D.F. & Graziano, M.S. (2004) Super-flinchers and nerves of steel: defensive movements altered by chemical manipulation of a cortical motor area. *Neuron*, **43**, 585-593.

Crutcher, M.D. & DeLong, M.R. (1984a) Single cell studies of the primate putamen. I. Functional organization. *Experimental brain research*, **53**, 233-243.

Crutcher, M.D. & DeLong, M.R. (1984b) Single cell studies of the primate putamen. II. Relations to direction of movement and pattern of muscular activity. *Experimental brain research*, **53**, 244-258.

Davare, M., Kraskov, A., Rothwell, J.C. & Lemon, R.N. (2011) Interactions between areas of the cortical grasping network. *Current opinion in neurobiology*, **21**, 565-570.

Decety, J. & Sommerville, J.A. (2003) Shared representations between self and other: a social cognitive neuroscience view. *Trends in cognitive sciences*, **7**, 527-533.

Falcone, R., Cirillo, R., Ferraina, S. & Genovesio, A. (2017) Neural activity in macaque medial frontal cortex represents others' choices. *Scientific reports*, **7**, 12663.

Fattori, P., Breveglieri, R., Bosco, A., Gamberini, M. & Galletti, C. (2017) Vision for Prehension in the Medial Parietal Cortex. *Cereb Cortex*, **27**, 1149-1163.

Fattori, P., Breveglieri, R., Raos, V., Bosco, A. & Galletti, C. (2012) Vision for action in the macaque medial posterior parietal cortex. *The Journal of neuroscience : the official journal of the Society for Neuroscience*, **32**, 3221-3234.

Fluet, M.C., Baumann, M.A. & Scherberger, H. (2010) Context-specific grasp movement representation in macaque ventral premotor cortex. *The Journal of neuroscience : the official journal of the Society for Neuroscience*, **30**, 15175-15184.

Fogassi, L., Ferrari, P.F., Gesierich, B., Rozzi, S., Chersi, F. & Rizzolatti, G. (2005) Parietal lobe: from action organization to intention understanding. *Science*, **308**, 662-667.

Fogassi, L., Gallese, V., Buccino, G., Craighero, L., Fadiga, L. & Rizzolatti, G. (2001) Cortical mechanism for the visual guidance of hand grasping movements in the monkey: A reversible inactivation study. *Brain : a journal of neurology*, **124**, 571-586.

Fogassi, L., Gallese, V., Fadiga, L., Luppino, G., Matelli, M. & Rizzolatti, G. (1996) Coding of peripersonal space in inferior premotor cortex (area F4). *Journal of neurophysiology*, **76**, 141-157.

Fogassi, L., Raos, V., Franchi, G., Gallese, V., Luppino, G. & Matelli, M. (1999) Visual responses in the dorsal premotor area F2 of the macaque monkey. *Experimental brain research*, **128**, 194-199.

Fuster, J. (2015) *The Prefrontal Cortex*.

Gallego, J.A., Perich, M.G., Miller, L.E. & Solla, S.A. (2017) Neural Manifolds for the Control of Movement. *Neuron*, **94**, 978-984.

Gallese, V., Fadiga, L., Fogassi, L. & Rizzolatti, G. (1996) Action recognition in the premotor cortex. *Brain : a journal of neurology*, **119 (Pt 2)**, 593-609.

Gallese, V., Murata, A., Kaseda, M., Niki, N. & Sakata, H. (1994) Deficit of hand preshaping after muscimol injection in monkey parietal cortex. *Neuroreport*, **5**, 1525-1529.

Gamberini, M., Fattori, P. & Galletti, C. (2015) The medial parietal occipital areas in the macaque monkey. *Visual neuroscience*, **32**, E013.

Gamberini, M., Passarelli, L., Fattori, P., Zucchelli, M., Bakola, S., Luppino, G. & Galletti, C. (2009) Cortical connections of the visuomotor parietooccipital area V6Ad of the macaque monkey. *The Journal of comparative neurology*, **513**, 622-642.

Gentilucci, M., Scandolara, C., Pigarev, I.N. & Rizzolatti, G. (1983) Visual responses in the postarcuate cortex (area 6) of the monkey that are independent of eye position. *Experimental brain research*, **50**, 464-468.

Gerbella, M., Belmalih, A., Borra, E., Rozzi, S. & Luppino, G. (2011) Cortical connections of the anterior (F5a) subdivision of the macaque ventral premotor area F5. *Brain structure & function*, **216**, 43-65.

Gerbella, M., Borra, E., Rozzi, S. & Luppino, G. (2016) Connections of the macaque Granular Frontal Opercular (GrFO) area: a possible neural substrate for the contribution of limbic inputs for controlling hand and face/mouth actions. *Brain structure & function*, **221**, 59-78.

Gerbella, M., Borra, E., Tonelli, S., Rozzi, S. & Luppino, G. (2013) Connectional heterogeneity of the ventral part of the macaque area 46. *Cereb Cortex*, **23**, 967-987.

Gerbella, M., Rozzi, S. & Rizzolatti, G. (2017) The extended object-grasping network. *Experimental brain research*, **235**, 2903-2916.

Giese, M.A. & Rizzolatti, G. (2015) Neural and Computational Mechanisms of Action Processing: Interaction between Visual and Motor Representations. *Neuron*, **88**, 167-180.

Grafton, S.T. (2010) The cognitive neuroscience of prehension: recent developments. *Experimental brain research*, **204**, 475-491.

Graziano, M.S. (1999) Where is my arm? The relative role of vision and proprioception in the neuronal representation of limb position. *Proceedings of the National Academy of Sciences of the United States of America*, **96**, 10418-10421.

Haggard, P. (2008) Human volition: towards a neuroscience of will. *Nature reviews. Neuroscience*, **9**, 934-946.

Hasson, U. & Frith, C.D. (2016) Mirroring and beyond: coupled dynamics as a generalized framework for modelling social interactions. *Philosophical transactions of the Royal Society of London. Series B, Biological sciences*, **371**.

He, S.Q., Dum, R.P. & Strick, P.L. (1993) Topographic organization of corticospinal projections from the frontal lobe: motor areas on the lateral surface of the hemisphere. *The Journal of neuroscience : the official journal of the Society for Neuroscience*, **13**, 952-980.

Herwik, S., Paul, O. & Ruther, P. (2011) Ultrathin silicon chips of arbitrary shape by etching before grinding. *Journal of microelectromechanical systems*, **20**, 791-793.

Hoshi, E. & Tanji, J. (2007) Distinctions between dorsal and ventral premotor areas: anatomical connectivity and functional properties. *Current opinion in neurobiology*, **17**, 234-242.

Isoda, M. & Hikosaka, O. (2007) Switching from automatic to controlled action by monkey medial frontal cortex. *Nature neuroscience*, **10**, 240-248.

Isoda, M. & Noritake, A. (2013) What makes the dorsomedial frontal cortex active during reading the mental states of others? *Frontiers in neuroscience*, **7**, 232.

Janssen, P. & Scherberger, H. (2015) Visual guidance in control of grasping. *Annual review of neuroscience*, **38**, 69-86.

Jeannerod, M., Arbib, M.A., Rizzolatti, G. & Sakata, H. (1995) Grasping objects: the cortical mechanisms of visuomotor transformation. *Trends in neurosciences*, **18**, 314-320.

Kaas, J.H. & Stepniewska, I. (2016a) Evolution of posterior parietal cortex and parietal-frontal networks for specific actions in primates. *The Journal of comparative neurology*, **524**, 595-608.

Kaas, J.H. & Stepniewska, I. (2016b) Evolution of posterior parietal cortex and parietal-frontal networks for specific actions in primates. *Journal of Comparative Neurology*, **524**, 595-608.

Kakei, S., Hoffman, D.S. & Strick, P.L. (2001) Direction of action is represented in the ventral premotor cortex. *Nature neuroscience*, **4**, 1020-1025.

Kaminski, J., Sullivan, S., Chung, J.M., Ross, I.B., Mamelak, A.N. & Rutishauser, U. (2017) Persistently active neurons in human medial frontal and medial temporal lobe support working memory. *Nature neuroscience*, **20**, 590-601.

Kandel, E.R.S., J.H.; Jessell, T.M.; Siegelbaum, S.A.; Hudspeth, A.J. (2012) *Principles of neural science*.

Kraskov, A., Prabhu, G., Quallo, M.M., Lemon, R.N. & Brochier, T. (2011) Ventral premotor-motor cortex interactions in the macaque monkey during grasp: response of single neurons to intracortical microstimulation. *The Journal of neuroscience : the official journal of the Society for Neuroscience*, **31**, 8812-8821.

Lanzilotto, M., Livi, A., Maranesi, M., Gerbella, M., Barz, F., Ruther, P., Fogassi, L., Rizzolatti, G. & Bonini, L. (2016) Extending the Cortical Grasping Network: Pre-supplementary Motor Neuron Activity During Vision and Grasping of Objects. *Cereb Cortex*, **26**, 4435-4449.

Lewis, J.W. & Van Essen, D.C. (2000) Corticocortical connections of visual, sensorimotor, and multimodal processing areas in the parietal lobe of the macaque monkey. *The Journal of comparative neurology*, **428**, 112-137.

Lucchetti, C., Lanzilotto, M., Perciavalle, V. & Bon, L. (2012) Neuronal activity reflecting progression of trials in the pre-supplementary motor area of macaque monkey: an expression of neuronal flexibility. *Neuroscience letters*, **506**, 33-38.

Luppino, G., Matelli, M., Camarda, R., Gallese, V. & Rizzolatti, G. (1991a) Multiple representations of body movements in mesial area 6 and the adjacent cingulate cortex: an intracortical microstimulation study in the macaque monkey. *Journal of Comparative Neurology*, **311**, 463-482.

Luppino, G., Matelli, M., Camarda, R. & Rizzolatti, G. (1993) Corticocortical connections of area F3 (SMA-proper) and area F6 (pre-SMA) in the macaque monkey. *The Journal of comparative neurology*, **338**, 114-140.

Luppino, G., Matelli, M., Camarda, R.M., Gallese, V. & Rizzolatti, G. (1991b) Multiple representations of body movements in mesial area 6 and the adjacent cingulate cortex: an intracortical microstimulation study in the macaque monkey. *The Journal of comparative neurology*, **311**, 463-482.

Macfarlane, N.B. & Graziano, M.S. (2009) Diversity of grip in Macaca mulatta. *Experimental brain research*, **197**, 255-268.

Maranesi, M., Bonini, L. & Fogassi, L. (2014a) Cortical processing of object affordances for self and others' action. *Frontiers in psychology*, **5**, 538.

Maranesi, M., Livi, A. & Bonini, L. (2015) Processing of Own Hand Visual Feedback during Object Grasping in Ventral Premotor Mirror Neurons. *The Journal of neuroscience : the official journal of the Society for Neuroscience*, **35**, 11824-11829.

Maranesi, M., Livi, A. & Bonini, L. (2017) Spatial and viewpoint selectivity for others' observed actions in monkey ventral premotor mirror neurons. *Scientific reports*, **7**, 8231.

Maranesi, M., Livi, A., Fogassi, L., Rizzolatti, G. & Bonini, L. (2014b) Mirror neuron activation prior to action observation in a predictable context. *The Journal of neuroscience : the official journal of the Society for Neuroscience*, **34**, 14827-14832.

Marconi, B., Genovesio, A., Battaglia-Mayer, A., Ferraina, S., Squatrito, S., Molinari, M., Lacquaniti, F. & Caminiti, R. (2001) Eye-hand coordination during reaching. I. Anatomical relationships between parietal and frontal cortex. *Cereb Cortex*, **11**, 513-527.

Matelli, M., Camarda, R., Glickstein, M. & Rizzolatti, G. (1986) Afferent and efferent projections of the inferior area 6 in the macaque monkey. *The Journal of comparative neurology*, **251**, 281-298.

Matelli, M., Luppino, G. & Rizzolatti, G. (1991) Architecture of superior and mesial area 6 and the adjacent cingulate cortex in the macaque monkey. *The Journal of comparative neurology*, **311**, 445-462.

Mazurek, K.A., Rouse, A.G. & Schieber, M.H. (2018) Mirror Neuron Populations Represent Sequences of Behavioral Epochs During Both Execution and Observation. *The Journal of neuroscience : the official journal of the Society for Neuroscience*, **38**, 4441-4455.

Meyers, E.M. (2013) The neural decoding toolbox. *Frontiers in neuroinformatics*, **7**, 8.

Moody, S.L. & Zipser, D. (1998) A model of reaching dynamics in primary motor cortex. *Journal of cognitive neuroscience*, **10**, 35-45.

Mukamel, R., Ekstrom, A.D., Kaplan, J., Iacoboni, M. & Fried, I. (2010) Single-neuron responses in humans during execution and observation of actions. *Current biology : CB*, **20**, 750-756.

Murata, A., Fadiga, L., Fogassi, L., Gallese, V., Raos, V. & Rizzolatti, G. (1997) Object representation in the ventral premotor cortex (area F5) of the monkey. *Journal of neurophysiology*, **78**, 2226-2230.

Nachev, P., Kennard, C. & Husain, M. (2008) Functional role of the supplementary and pre-supplementary motor areas. *Nature reviews. Neuroscience*, **9**, 856-869.

Nakajima, T., Hosaka, R., Mushiake, H. & Tanji, J. (2009) Covert representation of second-next movement in the pre-supplementary motor area of monkeys. *Journal of neurophysiology*, **101**, 1883-1889.

Nakamura, K., Sakai, K. & Hikosaka, O. (1998) Neuronal activity in medial frontal cortex during learning of sequential procedures. *Journal of neurophysiology*, **80**, 2671-2687.

Pandya, D.N. & Seltzer, B. (1982) Intrinsic connections and architectonics of posterior parietal cortex in the rhesus monkey. *The Journal of comparative neurology*, **204**, 196-210.

Parthasarathy, H.B., Schall, J.D. & Graybiel, A.M. (1992) Distributed but convergent ordering of corticostriatal projections: analysis of the frontal eye field

and the supplementary eye field in the macaque monkey. *The Journal of neuroscience : the official journal of the Society for Neuroscience*, **12**, 4468-4488.

Pezzulo, G. & Cisek, P. (2016) Navigating the Affordance Landscape: Feedback Control as a Process Model of Behavior and Cognition. *Trends in cognitive sciences*, **20**, 414-424.

Raos, V., Umilta, M.A., Gallese, V. & Fogassi, L. (2004) Functional properties of grasping-related neurons in the dorsal premotor area F2 of the macaque monkey. *Journal of neurophysiology*, **92**, 1990-2002.

Raos, V., Umilta, M.A., Murata, A., Fogassi, L. & Gallese, V. (2006) Functional properties of grasping-related neurons in the ventral premotor area F5 of the macaque monkey. *Journal of neurophysiology*, **95**, 709-729.

Rizzolatti, G., Camarda, R., Fogassi, L., Gentilucci, M., Luppino, G. & Matelli, M. (1988) Functional organization of inferior area 6 in the macaque monkey. II. Area F5 and the control of distal movements. *Experimental brain research*, **71**, 491-507.

Rizzolatti, G., Cattaneo, L., Fabbri-Destro, M. & Rozzi, S. (2014) Cortical mechanisms underlying the organization of goal-directed actions and mirror neuron-based action understanding. *Physiological reviews*, **94**, 655-706.

Rizzolatti, G., Fadiga, L., Gallese, V. & Fogassi, L. (1996) Premotor cortex and the recognition of motor actions. *Cognitive Brain Res*, **3**, 131-141.

Rizzolatti, G., Gentilucci, M., Camarda, R., Gallese, V., Luppino, G., Matelli, M. & Fogassi, L. (1990a) Neurons related to reaching-grasping arm movements in the rostral part of area 6 (area 6aβ). *Experimental brain research*, **82**, 337-350.

Rizzolatti, G., Gentilucci, M., Camarda, R.M., Gallese, V., Luppino, G., Matelli, M. & Fogassi, L. (1990b) Neurons related to reaching-grasping arm movements in the rostral part of area 6 (area 6a beta). *Experimental brain research*, **82**, 337-350.

Rizzolatti, G. & Luppino, G. (2001) The cortical motor system. *Neuron*, **31**, 889-901.

Rizzolatti, G. & Sinigaglia, C. (2016) The mirror mechanism: a basic principle of brain function. *Nature reviews. Neuroscience*, **17**, 757-765.

Rozzi, S., Calzavara, R., Belmalih, A., Borra, E., Gregoriou, G.G., Matelli, M. & Luppino, G. (2006) Cortical connections of the inferior parietal cortical convexity of the macaque monkey. *Cereb Cortex*, **16**, 1389-1417.

Rutishauser, U., Ye, S., Koroma, M., Tudusciuc, O., Ross, I.B., Chung, J.M. & Mamelak, A.N. (2015) Representation of retrieval confidence by single neurons in the human medial temporal lobe. *Nature neuroscience*, **18**, 1041-1050.

Sakata, H., Taira, M., Murata, A. & Mine, S. (1995) Neural mechanisms of visual guidance of hand action in the parietal cortex of the monkey. *Cereb Cortex*, **5**, 429-438.

Saleem, K.S., Miller, B. & Price, J.L. (2014) Subdivisions and connectional networks of the lateral prefrontal cortex in the macaque monkey. *The Journal of comparative neurology*, **522**, 1641-1690.

Schaffelhofer, S., Agudelo-Toro, A. & Scherberger, H. (2015) Decoding a wide range of hand configurations from macaque motor, premotor, and parietal cortices. *The Journal of neuroscience : the official journal of the Society for Neuroscience*, **35**, 1068-1081.

Schaffelhofer, S. & Scherberger, H. (2016) Object vision to hand action in macaque parietal, premotor, and motor cortices. *eLife*, **5**.

Serruya, M.D., Hatsopoulos, N.G., Paninski, L., Fellows, M.R. & Donoghue, J.P. (2002) Instant neural control of a movement signal. *Nature*, **416**, 141-142.

Shima, K. & Tanji, J. (2006) Binary-coded monitoring of a behavioral sequence by cells in the pre-supplementary motor area. *The Journal of neuroscience : the official journal of the Society for Neuroscience*, **26**, 2579-2582.

Simone, L., Rozzi, S., Bimbi, M. & Fogassi, L. (2015) Movement-related activity during goal-directed hand actions in the monkey ventrolateral prefrontal cortex. *The European journal of neuroscience*, **42**, 2882-2894.

Sinigaglia, C. & Rizzolatti, G. (2011) Through the looking glass: self and others. *Consciousness and cognition*, **20**, 64-74.

Sliwa, J. & Freiwald, W.A. (2017) A dedicated network for social interaction processing in the primate brain. *Science*, **356**, 745-749.

Takada, M., Tokuno, H., Hamada, I., Inase, M., Ito, Y., Imanishi, M., Hasegawa, N., Akazawa, T., Hatanaka, N. & Nambu, A. (2001) Organization of inputs from cingulate motor areas to basal ganglia in macaque monkey. *The European journal of neuroscience*, **14**, 1633-1650.

Tanji, J. (2001) Sequential organization of multiple movements: involvement of cortical motor areas. *Annual review of neuroscience*, **24**, 631-651.

Tanji, J. & Hoshi, E. (2001) Behavioral planning in the prefrontal cortex. *Current opinion in neurobiology*, **11**, 164-170.

Thaler, D., Chen, Y.C., Nixon, P.D., Stern, C.E. & Passingham, R.E. (1995) The functions of the medial premotor cortex. I. Simple learned movements. *Experimental brain research*, **102**, 445-460.

Umilta, M.A., Escola, L., Intskirveli, I., Grammont, F., Rochat, M., Caruana, F., Jezzini, A., Gallese, V. & Rizzolatti, G. (2008) When pliers become fingers in the monkey motor system. *Proceedings of the National Academy of Sciences of the United States of America*, **105**, 2209-2213.

van Schie, H.T., Mars, R.B., Coles, M.G. & Bekkering, H. (2004) Modulation of activity in medial frontal and motor cortices during error observation. *Nature neuroscience*, **7**, 549-554.

Vargas-Irwin, C.E., Franquemont, L., Black, M.J. & Donoghue, J.P. (2015) Linking Objects to Actions: Encoding of Target Object and Grasping Strategy in Primate Ventral Premotor Cortex. *The Journal of neuroscience : the official journal of the Society for Neuroscience*, **35**, 10888-10897.

Yoshida, K., Saito, N., Iriki, A. & Isoda, M. (2011) Representation of others' action by neurons in monkey medial frontal cortex. *Current biology : CB*, **21**, 249-253.

Yoshida, K., Saito, N., Iriki, A. & Isoda, M. (2012) Social error monitoring in macaque frontal cortex. *Nature neuroscience*, **15**, 1307-1312.

Zhang, Y., Meyers, E.M., Bichot, N.P., Serre, T., Poggio, T.A. & Desimone, R. (2011) Object decoding with attention in inferior temporal cortex. *Proceedings of the National Academy of Sciences of the United States of America*, **108**, 8850-8855.